Designing a 4-way metabolic junction

Brett Gareth Olivier

Thesis presented in partial fulfilment of the requirements for the degree of Master of Science (Biochemistry) at the University of Stellenbosch

Supervisor: Prof J-HS Hofmeyr
Co-supervisor: Dr JM Rohwer
August 1999

Printed on May 22, 2002

Declaration

I, the undersigned, declare that the work contained in this thesis is my own original work and has not previously in its entirety or in part been subjected to any university for a degree.

Signature

Date

Summary

Ultimately, understanding life at the molecular level is a question of reverse engineering, i.e., figuring out functions and how the design fulfills those functions. In the world of technology, experience in forward-engineering, i.e., designing a machine to do something, is usually a pre-requisite for success in reverse engineering similar machines. In order to gain such experience for becoming better reverse engineers of life, we set out to design (on paper) a metabolic system from scratch to perform a predefined set of functions. We chose a ubiquitous metabolic motif as example: the four-way junction around an internal 'end-product' such as an amino acid or a nucleotide. Such a metabolite stands at a crossroads of biosynthetic supply, external supply, consumption by internal demand (synthesis of macromolecules for maintenance and growth), and degradation by catabolic processes. In a nutshell, the system was designed to:

1. respond sensitively and rapidly to changes in the internal demand;
2. maintain the steady-state concentration of the end-product at a relatively low, far-from-equilibrium value;
3. switch off the biosynthetic supply when end-product is supplied from the external environment;
4. have the catabolic demand inoperative at end-product concentrations in the normal working range, but acting as an overflow valve when end-product increases for some reason, such as external oversupply.

Our main design tool was the log-log composite of rate characteristics, and we made extensive use of control analysis, enzyme kinetics, and computer simulation. Not only were we able to design the 4-way junction to conform to the set criteria, but we gained a deep understanding of the factors that determine functional differentiation in reactions networks.

Opsomming

Hoe ons lewe op 'n molekulêre vlak verstaan is uiteindelik 'n kwessie van tru-ingenieurswese, d.w.s., wat die funksies van sisteme is en hoe hul ontwerp hulle hierdie funksies laat verrig. In die wêreld van tegnologie is ondervinding van voorwaartse ingenieurswese, d.w.s, die ontwerp van 'n masjien om iets te doen, gewoonlik 'n voorvereiste vir sukses in tru-ingenieurswese van 'n soortgelyke masjien. Om sulke ondervinding op te doen sodat ons meer effektiewe 'tru-ingenieurs van lewe' kan word het ons onsself die taak gestel om vanuit basiese beginsels 'n metaboliese sisteem te ontwerp om 'n voorafbepaalde stel funksies te verrig. Die sisteem wat ons gekies het is 'n alomteenwoordige metaboliese motief: die 4-rigtingkruispad rondom 'n interne 'endproduk' soos 'n aminosuur of 'n nukleotied. So 'n endproduk staan op die kruispad van biosintetiese produksie, eksterne voorsiening, interne verbruik (deur sintese van makromolekule vir groei en instandhouding), en degradasie deur kataboliese prosesse. In kort is die sisteem ontwerp om:

1. sensitief en vinnig te reageer op veranderinge in interne verbruik;

2. die bestendige toestandskonsentrasie van die endproduk te handhaaf by 'n relatief lae, ver-van-ewewigswaarde;

3. die biosintetiese produksie af te skakel wanneer endproduk vanuit die eksterne omgewing voorsien word;

4. te sorg dat die kataboliese verbruik afgeskakel is by endprodukkonsentrasies in die normale werksgebied, maar dat dit as oorloopklep dien wanneer die endproduk toeneem vir een of ander rede, soos byvoorbeeld oorvoorsiening vanuit die omgewing.

Ons belangrikste ontwerphulpmiddel was die saamgestelde log-log snelheidskenmerkgrafieke, en ons het ook uitgebreid gebruik gemaak van kontrole analise, ensiemkinetika, en rekenaarsimulering. Nie net het ons daarin geslaag om die 4-rigtingkruispad te ontwerp om aan die gestelde kriteria te voldoen nie, maar ons het ook in die proses 'n diep begrip ontwikkel van die faktore wat funksionele differensiasie in reaksienetwerke bepaal.

For my parents and family

Acknowledgements

I would like to thank:

Prof Jannie Hofmeyr as supervisor and mentor for all the support without which this project would not have been realised, and for inspiring a deep and lasting interest in the subject of Biochemistry.

Dr Johann Rohwer as co-supervisor for always being available for essential encouragement and discussion.

Norbert Kolar, Nic Lombard, Tom Cunningham and Eugene Strauss, for the much valued friendship and support at any time of day or night.

The National Research Foundation and Harry Crossley Foundation for providing financial assistance during the course of my studies.

Contents

1 Introduction to metabolic design

1.1 Introduction

> In forward-engineering, one designs a machine to do something; in reverse-engineering, one figures out what a machine was designed to do. Reverse-engineering is what the boffins at Sony do when a new product is announced by Panasonic, or vice versa. They buy one, bring it back to the lab, take a screwdriver to it, and try to figure out what all the parts are for and how they combine to make the device work. We all engage in reverse-engineering when we face an interesting new gadget.
> Steven Pinker (1997) *How the mind works*, Penguin Books, London.

A living system is the ultimate 'interesting gadget'; anybody who has tried to understand life and the processes of life, whether at molecular or ecological or an in-between level, has invariably come up against the problem of having to do reverse-engineering. To paraphrase Steven Pinker: biochemists prepare a cell suspension in the lab, take a Waring blender to it, isolate and study all the parts, and try to figure out what they are for and how they combine to make a living cell. How successful have we been? In one sense, spectacularly successful. To a large degree, we have isolated and identified all the compounds that make up a living cell and figured out their properties, we know how they are made and degraded, we understand the kinetic properties of the enzymes that catalyse these interconversions, and we understand how the information for making the enzymes is stored, expressed and passed on to the next generation. We have also discovered a range of mechanisms for transducing extracellular information into intracellular information and for passing it around within the chemical pathways of the cell. We have therefore been good at figuring out what all the parts are for and how they communicate. What we have not been so good at is figuring out how they combine to make a cell 'live'. This, unfortunately, is the crucial part of reverse-engineering. The boffins at Sony may have figured out what each part of Panasonic's device is and does, but until they understand how the parts all combine to produce the 'emergent property' that makes the new device so exciting they cannot rest.

A question that is seldom asked is how one becomes an effective reverse-engineer. What experience must one have to make Sony want to employ you to reverse-engineer Panasonic's latest gadget? Obviously, the one crucial attribute is experience in designing devices similar or at least related to the one you are supposed to study. One would not expect Sony to employ a mechanical engineer to reverse-engineer Panasonic's latest

digital noise reduction filter, even though she may be adept at reverse-engineering new methods for fuel injection (unless they are totally stuck and in need of lateral thinking). However, whereas Sony could be expected to find the appropriate expertise, where does one find a biochemist who has experience in designing metabolic systems? The short answer to this is: virtually nowhere. The main reason for this is that reverse-engineering complex chemical networks depends absolutely on the existence of a quantitative language for describing the systemic behaviour of such networks. Such languages have been in existence for two or more decades: control analysis [1, 2] or biochemical systems theory [3] are the most highly developed. Nevertheless, very few biologists speak these languages, and even those who do are not necessarily experts in metabolic design. This thesis describes an attempt at gaining such expertise using an approach that is to our knowledge quite novel: we set out to design, from basic principles, a metabolic system that fulfils a predefined set of functions. We hope that this will allow us to understand the experimentally-determined properties of real examples of such systems.

The difference between our approach and the traditional approach to understanding metabolism is subtle, but nevertheless far-reaching. Usually, after the pathway structure has been determined experimentally, the component enzymes are kinetically characterised and only then is a function attributed to the system. Often, however, function exists only in the eye of the beholder, who is often biased by historical explanations and textbook views. Take glycolysis, for example. Depending on the angle from which it is approached, glycolysis can be seen as (i) a system for converting hexoses into pyruvate and, in yeast, into ethanol, (ii) a source of ATP through substrate level phosphorylation. From the first point of view glycolysis would be seen as a linear system that produces an end-product, or, more correctly, as a branched system, since certain intermediates of glycolysis lead to other products. From the second point of view glycolysis forms the ATP-producing half of a cycle which is closed by reactions that consume ATP. Much depends on the way the pathway is represented, and how much of the rest of the cellular process is taken into account. The real answer to the functional question must lie in the actual behaviour and performance of the system as it is challenged by changing external conditions (external to the system being studied, that is, and not necessarily extracellular; if we study a cellular subsystem, then the rest of the cell is part of the external environment of that system). Most often we find ourselves in a chicken-and-egg situation: we need to judge performance in terms of functional criteria, but, traditionally, we had to guess at the function by observing the performance. The approach followed in this thesis avoids this problem. We start out by specifying functional criteria, then we design for and judge performance by those criteria.

We shall proceed as follows: in the next section we distill from the complex web of metabolic interactions a basic set of structural motifs and choose one of them, the 4-way metabolic junction, as our target. Our aim then is to design a generic 4-way junction according to a set of pre-defined functional criteria which we believe most biochemists will accept as realistic. The design process will generate a set of theoretically required system properties that can be compared with real experimentally-determined system properties. A closeness of the match should give an indication of how realistic the criteria were in the first place. In this process we may also discover behavioural properties which

do not match our criteria, but could be useful for fulfilling other possible criteria.

1.1.1 Structural motifs in metabolism

The metabolism of a cell at first seems complex and intangible. However, taking a step back and looking again, one begins to notice intricate patterns and motifs [4] (see Fig. 1.1).

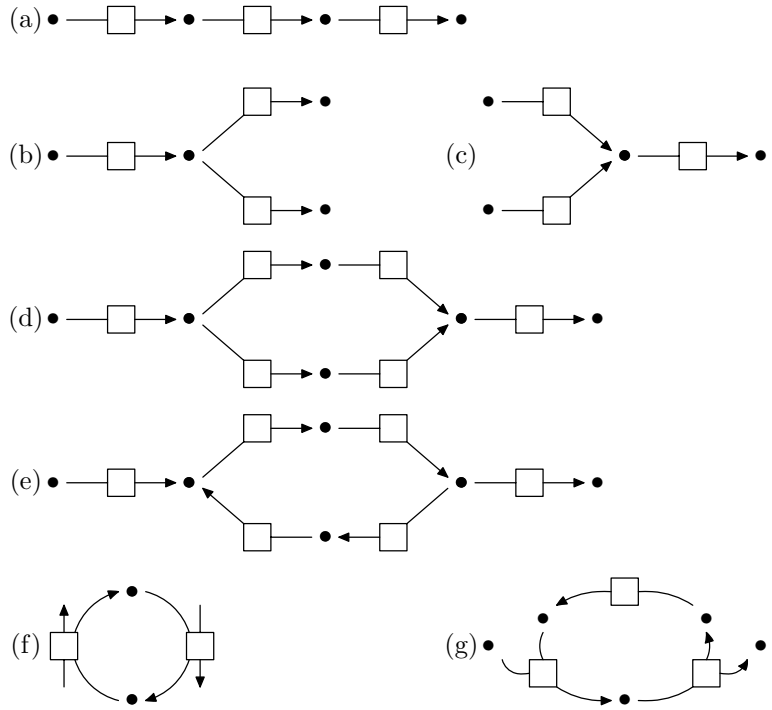

Fig. 1.1 *Motifs in metabolic pathways.* a linear chain; b diverging branch; c converging branch; d parallel loop; e anti-parallel loop (substrate cycle); f 2-member moiety-conserving cycle; g 3-member moiety-conserving cycle. Dots represent metabolites; boxes with arrows represent reactions or transport steps.

There are stretches of linear sequences where one step produces a metabolite and the next step consumes it; there are branchpoints where more than one step either forms or consumes a metabolite; sometimes branches reconverge to form parallel or antiparallel loops; reactions that interconvert two forms of a cofactor form cyclic structures. These motifs form the building blocks of metabolic pathways. Already at this early stage, a cautionary note should be sounded: metabolic pathways as traditionally depicted are incomplete in that important processes are left out. For example, amino acids and nucleotides are consumed by the processes of protein synthesis and nucleic acid synthesis, but metabolic maps usually do not show these processes explicitly. Only the synthetic process that leads to such a metabolite and the degradative processes that catabolise the metabolite are generally shown, giving the impression of a linear pathway through

the metabolite. If, however, processes such as macromolecular synthesis are taken into account, the branched motif is a more appropriate structural description.

1.1.2 The 4-way metabolic junction

Much of metabolism exists to synthesise building blocks for macromolecular synthesis. Such a building block therefore forms the link between a *biosynthetic supply* pathway and a growth process that we shall call the *internal demand* (Fig. 1.2 a).

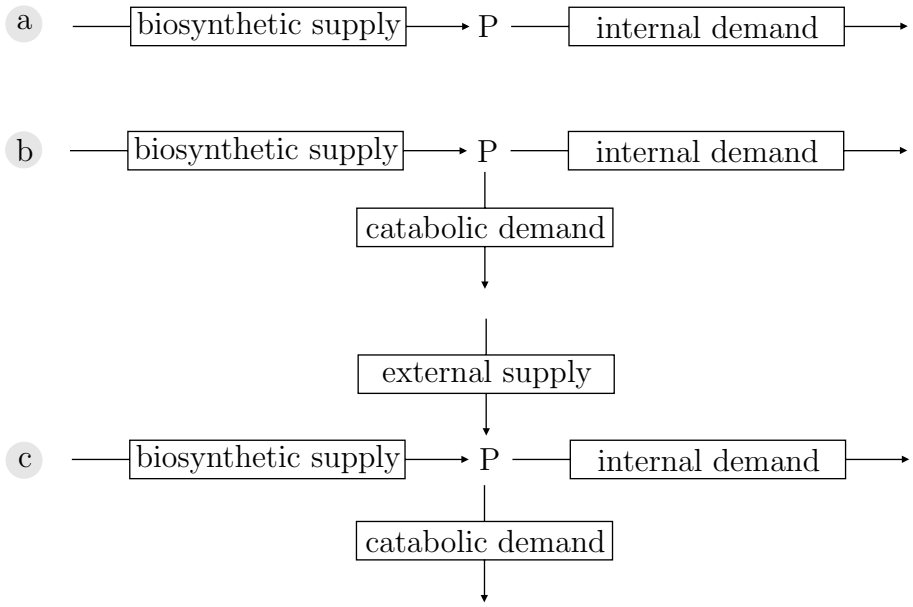

Fig. 1.2 *Building a 4-way metabolic junction.* a The core is a simple linear system consisting of a biosynthetic supply and an internal demand. b Including catabolic demand creates a 3-way junction. c Including external supply completes the 4-way junction. The boxes represent the different conversion blocks, with P the linking metabolite.

In addition there usually exists a *catabolic demand* that degrades the building block to make it available to energy metabolism. If this is taken into account the linear motif in Fig. 1.2 a is now seen to be a branched motif (Fig 1.2 b). Many cells also possess uptake systems for these building blocks, which, if they occur in the extracellular medium, can serve as the *external supply*. This extra supply branch changes the system into what we shall call a *4-way metabolic junction* with the generic structure depicted in Fig 1.2 c. It is this ubiquitous motif that we choose as a subject for metabolic design. The degree of behavioural complexity required for this system to function under a varied set of conditions make it a real challenge; this is the main reason for our choice. Another reason is that the biosynthetic supply block is often subject to end-product inhibition, a regulatory mechanism about which much experimental information is available and that has been studied using the formalism of control analysis [5]. As an added bonus, this affords us the opportunity to evaluate the newly developed reversible Hill-mechanism

for cooperative enzymes with modifiers [6] as a tool for modelling and predicting the behaviour of feedback systems.

The 4-way junction as described above is rather abstract. To make it more real it is instructive to describe a specific example of such a junction. The obvious candidates for end-products around which such junctions exist are amino acids and nucleotides. We choose isoleucine in *Escherichia coli* as a representative example (in deference to its status as the first amino acid discovered to act as feedback inhibitor of the first enzyme in its biosynthetic sequence [7]). As shown in Fig. 1.3, isoleucine is produced biosynthetically and consumed during protein synthesis, it is catabolically degraded and can be transported into the cell (details are given in the figure legend). As always reality seldom conforms to simple generic schemes: except for threonine deaminase, the first enzyme in the isoleucine sequence, the other biosynthetic enzymes catalyse the corresponding steps in the production of valine. However, as we are not interested in duplicating a specific example of a 4-way junction, this is of little importance.

1.2 What every metabolic designer should know

1.2.1 A metabolic designer's toolbox

To successfully design metabolic systems for function we need the right tools. We have found the following to be indispensable components of the metabolic designer's toolbox.

1. The quantitative framework known as *control analysis*, developed from the pioneering work of Kacser and Burns (see [1] for an updated version of their original paper) and Heinrich and Rapoport [2], is used to describe the mathematical relationships between the kinetic properties of the steps of the system and the control properties of the system as a whole.

2. Classical *enzyme kinetics* [8] is necessary for describing the properties of individual enzymes in terms of rate equations.

3. Understanding is often, if not always, enhanced by a good graphical depiction of a concept or relationship. We have found so-called *rate characteristics* [9] to be extremely useful for understanding not only the behaviour around a specific steady state, but also the behaviour over large ranges of parameter values. A related graphical representation of system behaviour in terms of *parameter portraits* is a suitable adjunct to rate characteristics. The free graphics program Gnuplot was used to plot these graphs. Another excellent tool is Herbert Sauro's Vexplorer (ftp://bmsdarwin.brookes.ac.uk/pub/mca/software/ibmpc/explorer/). This utility draws 'live' graphs, in the sense that the graph of an algebraic function changes dynamically as one of its parameters is dragged between two limits.

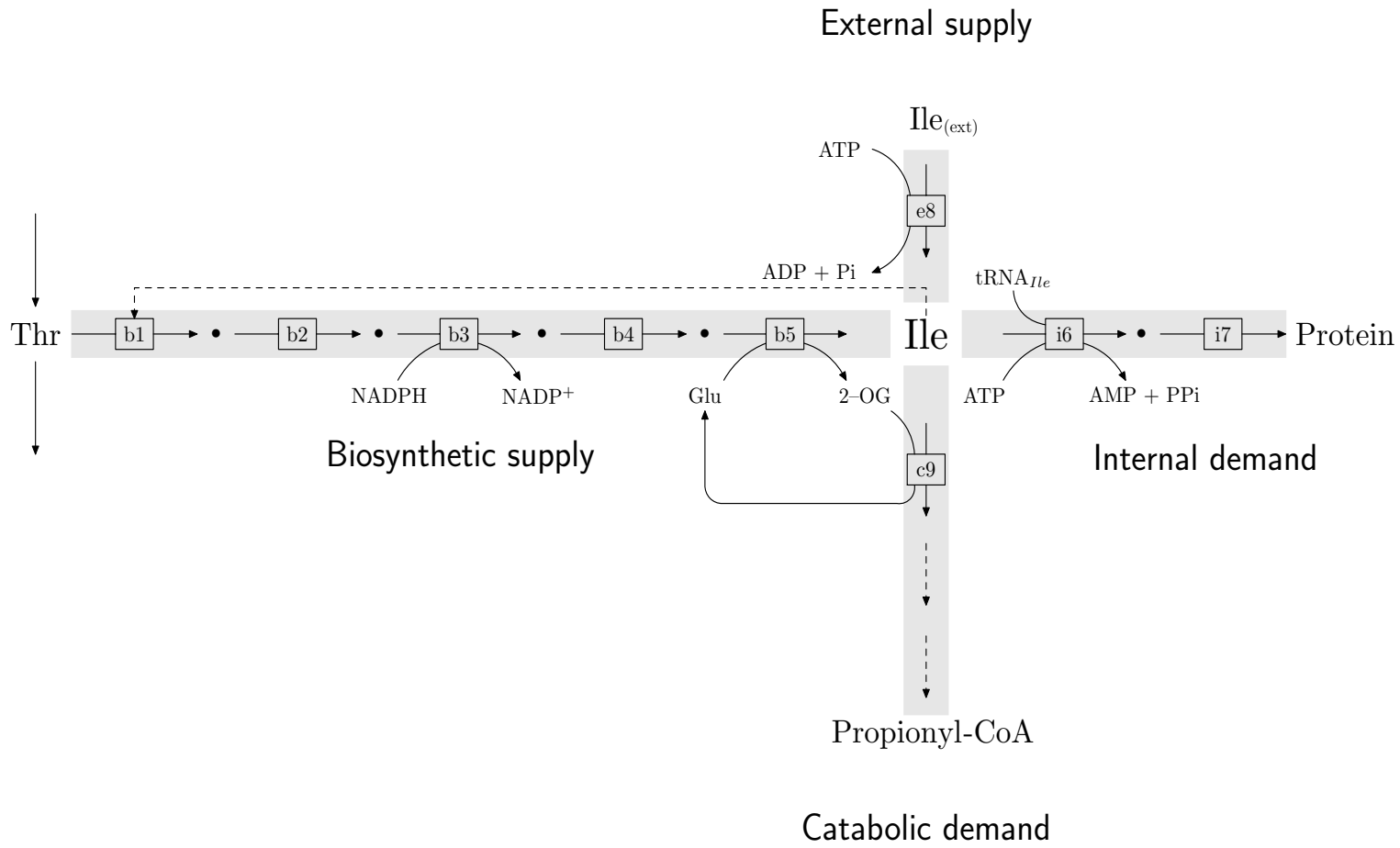

Fig. 1.3 *Isoleucine metabolism as an example of a 4-way metabolic junction.* The boxes represent enzymes, and dots, metabolites. Biosynthetic supply: Threonine deaminase **(b1)** converts threonine to α-ketobutyrate, which is then converted to α-aceto-α-hydroxybutyrate by acetohydroxy acid synthase **(b2)**. Acetohydroxy acid isomerase **(b3)** converts α-aceto-α-hydroxy butyrate into α,β-dihydroxy-β-methylvalerate, which is converted by dihydroxy acid dehydrase **(b4)** into α-keto-β-methylvalerate. Branched-chain amino acid glutamate transaminase **(b5)** performs the final conversion into isoleucine. A dashed line shows inhibition of **(b1)** by Ile. Internal demand: Isoleucine is linked to an Ile specific tRNA by aminoacyl-tRNA synthetase **(i6)** to form isoleucyl-tRNA, which is then available for protein synthesis **(i7)**. External supply: An ATP-dependent transporter **(e8)** imports Ile into the cell from the extracellular environment. Catabolic demand: Isoleucine is catabolised to propionyl-CoA by a branched-chain amino acid aminotransferase **(c9)**, the same as **(b5)**, and five more enzymes represented by the dashed arrows.

4. Finally, but most importantly, computer tools for numerically solving transients and steady states of reaction networks are indispensable for studying the behaviour of model reaction networks. We used Scamp [10] (a new WinScamp is also under development at http://members.tripod.co.uk/sauro/biotech.htm) or Gepasi [11] (version 3.21 is available at http://gepasi.dbs.aber.ac.uk/softw/gepasi.html).

1.2.2 Functions in reaction networks

Dynamically, reaction networks can exist in three possible states: transient, steady state, and equilibrium. Although only closed systems can reach equilibrium, thereby excluding it as a possible state for open living systems, it is important as a reference state: the distance ρ of any reaction or reaction block from equilibrium, defined as Γ/K_{eq}, where Γ is the mass-action ratio and K_{eq} is the equilibrium constant, is an important factor in determining the behaviour of any reaction network. Whereas equilibrium is the final state for closed systems, open systems tend towards a steady state, and are therefore either in this state or in a transient state which is moving towards the steady state. This is of course a gross simplification: a particular steady state can only be approached when the set of parameters that determine that state remain constant. In real life this is never so: parameters are constantly adjusted as the system responds to its environment. Nevertheless, experimental conditions can be set up in such a way that the system under study can be regarded as being in the steady state (an organism in a chemostat is a good example).

What is the 'function' of a reaction or reaction block in a reaction network? As explained in the introduction, the answer to this question is by no means clear-cut. For example, the question "What is the function of enzyme X?" can have several equally reasonable answers: To catalyse reaction X; to commit flux to a particular branch (if enzyme X occurs at a branchpoint); to (partly) control some metabolic flux or intermediate concentration; etc. Clearly, 'function' is a multi-level concept. We therefore have to be very specific about what we consider as function for the purpose of our design exercise. In general, the type of low-level functions that we shall use to assess the efficacy with which higher level functions are performed are all associated with aspects of the steady and transient state:

1. the determination of the level of a steady state flux or intermediate concentration (the steady state itself);

2. how a steady state flux or intermediate concentration responds to a small change in some system parameter (control of or structural stability of the steady state);

3. how a steady state flux or intermediate concentration responds to a large change in some system parameter (response profile);

4. how a steady state responds to a fluctuation in some intermediate concentration (dynamic stability of the steady state);

5. how long it takes to move from one steady state to another (transition time);

6. the dynamic form of the transition from one steady state to another (smooth monotonic, over or undershoot, damped oscillations, sustained oscillations, chaotic).

1.3 From factory analogy to reaction network

The economics of a factory forms an excellent analogy for developing the background for our design, and has been used productively by others (cf. [12]). Fig. 1.4 depicts the essence of a factory and its relationship to its environment in highly simplified form.

Fig. 1.4 *A schematic representation of a factory and its clients.* The factory supplies a product that fulfils the demand created by the consumers of that product.

In the context of the design of the factory, we can ask three basic questions:

1. What does the factory do? More generally, for any system, what is its *function*? Answer: The factory makes a product to be consumed by its clients.

2. How well does the factory fulfil its function? More generally, how can one measure the *performance* of a system in terms of its function? Answer: The factory

   a) must satisfy a range of demand;

   b) must respond rapidly enough to ensure this;

   c) should not accumulate product when demand is low.

3. What can the designers do to make it perform better (fulfil its function better)? More generally, how can they *regulate* its performance? Answer: By moulding the properties of the system components to achieve the desired effect. This then is also our working definition of the concept of regulation: to regulate something is to change its properties so that it behaves differently.

The factory analogy translates easily to the supply-demand system that forms the basis of our 4-way junction. Biosynthetic supply and internal demand correspond to the blocks in our simple figure of the factory (1.4). External supply can be thought of as ready-made product that the factory could temporarily obtain more cheaply than it would cost to produce it itself (adding the performance criterion that the internal supply should switch off automatically when such external supply is present). Catabolic demand can be thought of as an additional outlet for product should it accumulate in the factory for some reason (adding the performance criterion that this outlet should be closed under normal operating conditions).

From the metabolic designer's point of view, the important question is how the properties of the system components can be moulded to increase functional performance. Consider that, in the absence of any such regulation, a reaction network still has its own intrinsic mass-action behaviour, purely because it is a system of chemical reactions. We need to understand this intrinsic behaviour, because it is this behaviour that we want to change (regulate). Hofmeyr [9] has used this as a basis for our present definition of regulation:

> Taking open uncatalysed reaction networks as a starting point we see that mass-action is the main driving force for self-organisation. This is not to say that the behaviour of these systems is necessarily simple; for instance, non-enzymic networks can contain autocatalytic cycles that cause oscillations or deterministic chaos, multiple steady states, trigger behaviour. However, by identifying mass-action as the basic driving force, we can broadly define metabolic regulation as *the alteration of reaction properties to augment or counteract the mass-action trend in a network of reactions*. On the basis of our current knowledge, living systems have achieved this on two levels: *first*, by evolving (i) enzymes with high catalytic and binding specificity, (ii) mechanisms for altering enzyme activity, concentration and binding properties, and (iii) allosteric and other signals; *second*, by evolving special stoichiometric network structures such as moiety-conserved and autocatalytic cycles. Without the evolution of enzymes this moulding process would have been impossible: on the one hand, enzymes lift the metabolic network from the underlying network of thermodynamically feasible reactions onto a different timescale; on the other, enzymes add controllability and regulability to metabolism—without enzymes evolution would have had no 'handles' to work with [9].

It is possible to quantify this definition of regulation [9]. Control analysis has shown that the reaction properties of importance for understanding steady-state responses to perturbations in any parameter are the so-called elasticity coefficients of the rate with respect to any chemical species that is directly involved in the reaction (i.e., a substrate, product, or any effector that binds to the enzyme in the case of an enzyme-catalysed reaction). In general, the rate of a chemical reaction such as $a\mathrm{A} + b\mathrm{B} \rightleftharpoons c\mathrm{C} + d\mathrm{D}$ can be written as

$$\begin{array}{ccccccc} v & = & \Theta & \cdot & k_\mathrm{f} & \cdot & \left(A^a B^b - \dfrac{C^c D^d}{K_\mathrm{eq}}\right) \\ & & \text{Kinetic function of A, B, C and D} & & \text{Intrinsic rate constant} & & \text{Thermodynamic mass-action term} \end{array}$$

Differentiating the logarithmic form of the rate equation with respect to the logarithm of any species in the rate equation yields the algebraic expression for any elasticity [9]. For the general rate equation given above, representative expressions for substrate and

product elasticity coefficients would be:

$$\varepsilon_a^v = \frac{\partial \ln v}{\partial \ln a} = \frac{\partial \ln \Theta}{\partial \ln a} + \frac{1}{1 - \frac{\Gamma}{K_{eq}}} \tag{1.1}$$

$$\varepsilon_c^v = \frac{\partial \ln v}{\partial \ln c} = \frac{\partial \ln \Theta}{\partial \ln c} - \frac{\frac{\Gamma}{K_{eq}}}{1 - \frac{\Gamma}{K_{eq}}} \tag{1.2}$$

The expression for the derivatives of Θ depend on its functional form. For example, when differentiation the reversible Michaelis-Menten rate equation for the reaction $\mathrm{S} \rightleftharpoons \mathrm{P}$

$$v = \frac{V_f}{K_s} \cdot \frac{1}{1 + \frac{s}{K_s} + \frac{p}{K_p}} \cdot \left(s - \frac{p}{K_{eq}} \right) \tag{1.3}$$

leads to the elasticity expressions

$$\varepsilon_s^v = \frac{\partial \ln v}{\partial \ln s} = \frac{-\frac{s}{K_s}}{1 + \frac{s}{K_s} + \frac{p}{K_p}} + \frac{1}{1 - \frac{\Gamma}{K_{eq}}} \tag{1.4}$$

$$\varepsilon_p^v = \frac{\partial \ln v}{\partial \ln p} = \frac{-\frac{p}{K_p}}{1 + \frac{s}{K_s} + \frac{p}{K_p}} - \frac{\frac{\Gamma}{K_{eq}}}{1 - \frac{\Gamma}{K_{eq}}} \tag{1.5}$$

The $\frac{\Gamma}{K_{eq}}$-containing terms are *thermodynamic*: they quantify the mass-action contribution to the sensitivity of reaction rate with respect to changes in substrate or product concentration. The other terms are depend on the reaction mechanism and are therefore *kinetic*; they augment or counteract the mass-action term and are therefore the key to quantifying regulation as defined above. If the reaction were uncatalysed its rate would be governed by mass-action only and the reaction would be unregulated; the kinetic terms would vanish, leaving only the thermodynamic terms in the elasticity expressions.

We as designers cannot change the thermodynamic properties of a reaction; we only have access to the rate constants and other kinetic parameters such as Michaelis constants, Hill-coefficients, enzyme concentration, etc. that appear in the kinetic term Θ.

1.4 Functional performance criteria for the 4-way junction

As in any engineering design project, the first step is to draw up the specifications of the system that will ultimately serve as criteria by which performance of the design can be tested. Here we just describe the specifications in broad terms; during the

actual design process they will be refined and quantified. As with most design processes the choice of specifications is informed by prior experience and knowledge, so that the following functional criteria are by no means arbitrary; in general terms they match the functions that biochemists currently accept as applicable to metabolic systems. We refer to metabolite P (which we have also described as the 'building block' or 'end-product') as the *linking metabolite*.

1. The system must respond *sensitively* to changes in the internal demand (synthesis of macromolecules for maintenance and growth). In other words, the internal demand must control its own flux completely or to a very high degree, at least within a specified range of variation. This is the primary and most basic functional criterion. In our system, the biosynthetic pathway exists solely to produce its 'end-product' for macromolecular synthesis, and must be able to cope with variation of internal demand within a set working range (Chapter 2).

2. The steady-state concentration of the linking metabolite P (and the other intermediates) should be maintained homeostatically at a low, far-from-equilibrium value. The limited solvent capacity of the cell for its thousands of molecular species requires that metabolites do not build up to high concentrations [13] (Chapter 3).

3. The system must respond *rapidly* to changes in the internal demand. This criterion is intimately linked to the previous one in that large pool sizes also tend to make the response of the system to perturbations sluggish [14] (Chapter 5).

4. The catabolic demand should not operate at concentrations of P in the normal working range, but should act as an overflow valve when P increases for some reason, such as external oversupply of P or extremely low demand for P. This would allow externally supplied P to be used as a source of energy (Chapter 6).

5. Biosynthetic supply should be switched off if P can be supplied from the external environment. The intuitive argument that lies at the basis of this criterion is that this should save on energy and reducing power usually needed for the biosynthesis of P (Chapter 6).

With this background the stage is set for our journey through the relatively unexplored territory of metabolic design.

2 Control properties of supply-demand systems

The deficiencies of the classical views on metabolic control and regulation have been well documented (e.g. [15]). However, the bulk of these discussions have centred on the problems engendered by the concept of a rate-limiting step, and perhaps rightly so. Less has been said about an even more serious deficiency, namely the way in which boundaries have been drawn around pathways in order to simplify description of the tangled web that is metabolism. Hofmeyr [16] explains this using yeast glycolysis as an example:

> The traditional textbook description of a metabolic pathway such as fermentative glycolysis in yeast is based on the net reaction
>
> $$\text{glucose} + 2\text{ADP} + 2\text{P}_\text{i} \longrightarrow 2\text{ethanol} + 2\text{CO}_2 + 2\text{ATP}$$
>
> There is, however, an important difference between glucose, ethanol, and CO_2 on the one hand, and ADP and ATP on the other. The first are 'external' substrates and products in the sense that they are ingested or excreted; they form natural metabolic boundaries. The second are 'internal' substrates and products; they form artificial metabolic boundaries at which the metabolic pathway connects with other cellular processes. So, what we call an 'end-product' is often the substrate for other cellular processes, e.g., ATP for biosynthesis and growth, amino acids for protein synthesis, nucleotides for nucleic acid synthesis. In principle there is of course nothing wrong with compartmenting a complex network into separate modules for purposes of analysis, whether experimental or theoretical. A problem arises, however, when the internal boundaries are carried over into an analysis of control and regulation. The reason is that while one or more steps in any module may exercise a high degree of control of some steady-state variable in the module when it is studied in isolation, it is possible that they lose that control completely when the system is expanded to include other connecting modules; this will happen when the module as a whole has little control over that variable within the expanded system (that this is a fundamental result from metabolic control analysis has not exempted control analysts from sometimes making the same mistake). The surprise caused by the failure of over-expressed glycolytic enzymes to affect flux can be largely ascribed

to an unfulfilled expectation that the control profile obtained for the glycolytic module in isolation can be extrapolated to the whole system of which glycolysis is part.

This has direct relevance for the 4-way junction. The product P would, in the classical view, be described as an 'end-product' feeding back onto the first 'rate-limiting' step of the biosynthetic pathway. This implies that the flux through the biosynthetic pathway is controlled by this first enzyme. If the biosynthetic pathway were to be analysed in isolation, this may very well turn out to be true. However, in the light of the factory analogy, it would make no functional sense if this were also true in the complete system which includes the demand for P. In fact, from a functional point of view one would expect no control in the supply, and all control in the demand [5, 16, 17]. This also makes sense from an evolutionary point of view: a system that meets the demand effectively should outcompete one that does not.

This again underpins the first functional criterion that we want to design for and which is paraphrased here:

The system must respond *sensitively* to changes in the internal demand, i.e., the internal demand must control its own flux completely or to a very high degree, at least within a working range of variation. In our system, the biosynthetic pathway exists solely to produce its 'end-product' for macromolecular synthesis, and must be able to cope with variation of internal demand within this working range.

2.1 Ensuring flux-control by demand

We need to know which properties of the supply-demand system determine the degree to which the supply and demand blocks control the flux and the concentration of P. At this stage we are not concerned with the details of the individual reactions within the blocks, and therefore take the bird's-eye view depicted in Fig. 2.1.

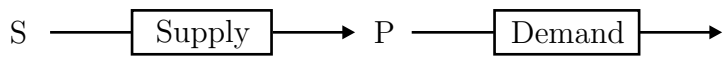

Fig. 2.1 *The basic supply-demand system for product P.*

A control analysis of this system [5] yields expressions for control coefficients in terms of elasticities of supply and demand. The flux-control coefficients are

$$C^J_{\text{supply}} = \frac{\varepsilon_p^{v_{\text{demand}}}}{\varepsilon_p^{v_{\text{demand}}} - \varepsilon_p^{v_{\text{supply}}}} = \frac{1}{1 - \dfrac{\varepsilon_p^{v_{\text{supply}}}}{\varepsilon_p^{v_{\text{demand}}}}} \tag{2.1}$$

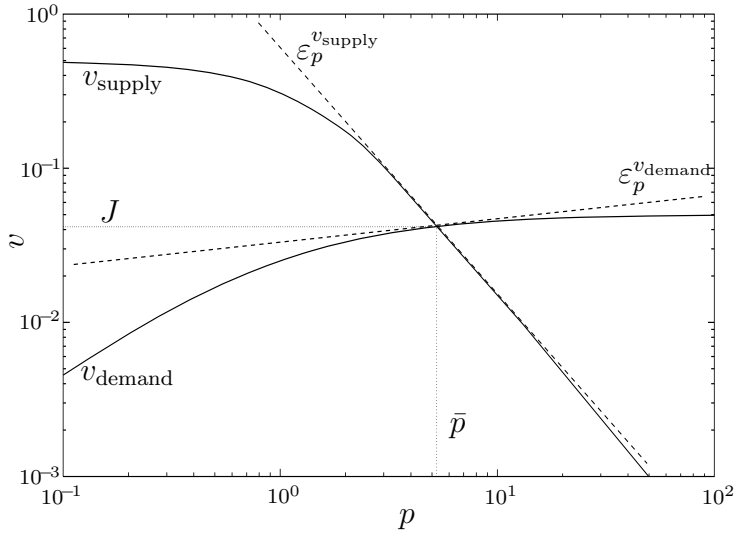

Fig. 2.2 *The rate characteristics of a supply-demand system plotted in log-log space.* Steady state obtains at the intersection point. At any p the slopes of the tangents of the rate curves are the elasticity coefficients of supply and demand at that particular value of p. Shown on the graph are the elasticities of supply and demand with respect to the linking metabolite P at steady state.

and

$$C^J_{\text{demand}} = \frac{-\varepsilon_p^{v_{\text{supply}}}}{\varepsilon_p^{v_{\text{demand}}} - \varepsilon_p^{v_{\text{supply}}}} = \frac{-\dfrac{\varepsilon_p^{v_{\text{supply}}}}{\varepsilon_p^{v_{\text{demand}}}}}{1 - \dfrac{\varepsilon_p^{v_{\text{supply}}}}{\varepsilon_p^{v_{\text{demand}}}}} \tag{2.2}$$

and the concentration-control coefficients:

$$C^p_{\text{supply}} = \frac{1}{\varepsilon_p^{v_{\text{demand}}} - \varepsilon_p^{v_{\text{supply}}}} \tag{2.3}$$

and

$$C^p_{\text{demand}} = \frac{-1}{\varepsilon_p^{v_{\text{demand}}} - \varepsilon_p^{v_{\text{supply}}}} \tag{2.4}$$

The ratio of elasticities determines the distribution of flux-control between supply and demand (the higher $-\varepsilon_p^{v_{\text{supply}}}/\varepsilon_p^{v_{\text{demand}}}$, the higher the flux-control by demand), while the sum of elasticities determines concentration control (the higher $\varepsilon_p^{v_{\text{demand}}} - \varepsilon_p^{v_{\text{supply}}}$, the smaller the absolute values of both C^p_{supply} and C^p_{demand}).

These relationships are clearly illustrated when the supply and demand rate dependencies on p are plotted on a graph of $\ln v$ against $\ln p$ (Fig. 2.2, a graph known as a composite *log-log rate characteristic* [9]).

The steady state obtains where the rate characteristics intersect. The slopes of the rate curves are equal to the elasticity coefficients of supply and demand, which are by definition

$$\varepsilon_p^{v_{\text{supply}}} = \frac{\partial \ln v_{\text{supply}}}{\partial \ln p} \qquad \text{and} \qquad \varepsilon_p^{v_{\text{demand}}} = \frac{\partial \ln v_{\text{demand}}}{\partial \ln p} \tag{2.5}$$

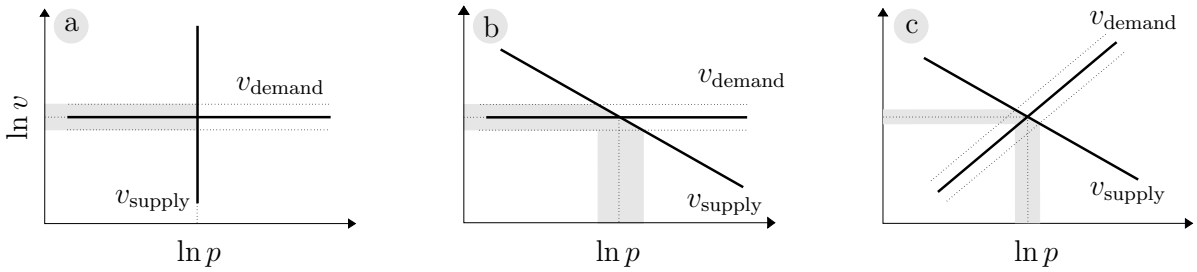

Fig. 2.3 *Tangents to log-log rate characteristics of supply and demand around the steady state.* Each line represents the slope of the tangent to a rate characteristic at the steady state, i.e., $\varepsilon_p^{v_{\text{supply}}}$ or $\varepsilon_p^{v_{\text{demand}}}$. The three graphs depict different configurations of elasticities. The dotted lines depict the same (small) percentage increase or decrease in demand activity. The shaded regions allow the effects on the steady-state flux (horizontal) and concentration of P (vertical) of this variation in demand activity to be compared.

To explore the implications of different constellations of supply and demand elasticities we compare three hypothetical situations (Fig. 2.3).

Graph a shows the extreme situation where $\varepsilon_p^{v_{\text{demand}}} = 0$ and $\varepsilon_p^{v_{\text{supply}}} \to -\infty$. If demand activity is varied (the shaded horizontal band) flux changes proportionally but $\bar{p}$ remains constant. It is clearly the zero demand elasticity that confers flux-control on the demand. If we exchanged the identities of the supply and demand rate curves, the supply elasticity would be zero and supply would have complete control over the flux. It is also apparent that the infinitely high supply elasticity that causes $\bar{p}$ to remain constant while the flux varies with demand. That the supply elasticity determines how much $\bar{p}$ changes when demand controls the flux, is emphasised by graph b where the $\varepsilon_p^{v_{\text{supply}}}$ has a less extreme value, but $\varepsilon_p^{v_{\text{demand}}}$ is still zero: variation in demand now does change $\bar{p}$ (the vertical shaded band) but the magnitude of the change is completely determined by the supply elasticity. If demand elasticity is not zero (graph c), demand loses some flux control (supply gains some flux control) and $\bar{p}$ becomes more resistant to change (more homeostatic).

Another important feature of such systems which is not immediately apparent is that when one block completely controls the flux, the other completely determines the actual value of the steady-state concentration of P. This follows from the assumption that $\varepsilon_p^{v_{\text{demand}}} \ll -\varepsilon_p^{v_{\text{supply}}}$ so that $C^J_{\text{demand}} \to 1$ and $C^p_{\text{demand}} = -C^p_{\text{supply}} \to 1/\varepsilon_p^{v_{\text{supply}}}$. Clearly concentration control here depends only on supply properties.

Therefore, to satisfy the criterion that requires flux control by demand we must ensure that $\varepsilon_p^{v_{\text{demand}}} \ll -\varepsilon_p^{v_{\text{supply}}}$. In practice, this can be achieved by saturating the demand with P, so that $\varepsilon_p^{v_{\text{demand}}} \to 0$. It is also clear at this stage that the second design requirement of homeostatic maintenance of $\bar{p}$ in the face of flux-control by demand will depend on the properties of the supply. We shall turn to this second phase of the design process in Chapter 3. In the rest of this chapter we shall extend the above analysis to encompass the full 4-way junction and discuss the implication for rate characteristic analysis of such a system.

2.2 Supply-demand analysis of the 4-way junction

Control analysis of the complete 4-way junction, shown again in Fig. 2.4, gives seemingly more complex expressions for flux-control coefficients.

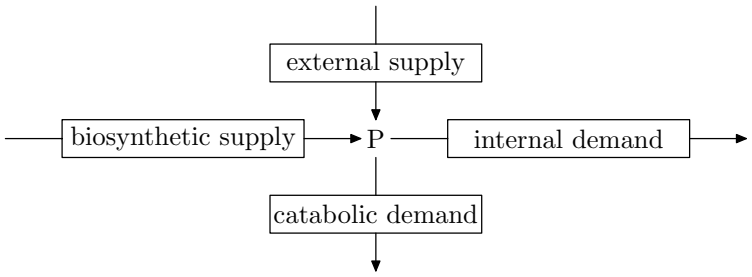

Fig. 2.4 *The 4-way metabolic junction.*

The following are the J_{dem}-control coefficient expressions (for the sake of clarity, we abbreviate the names of the four blocks):

$$C_{\text{bio}}^{J_{\text{dem}}} = \frac{\frac{J_{\text{bio}}}{J_{\text{dem}}}\varepsilon_p^{v_{\text{dem}}}}{\varepsilon_p^{v_{\text{dem}}} + \frac{J_{\text{cat}}}{J_{\text{dem}}}\varepsilon_p^{v_{\text{cat}}} - \frac{J_{\text{bio}}}{J_{\text{dem}}}\varepsilon_p^{v_{\text{bio}}} - \frac{J_{\text{ext}}}{J_{\text{dem}}}\varepsilon_p^{v_{\text{ext}}}} \tag{2.6}$$

$$C_{\text{ext}}^{J_{\text{dem}}} = \frac{\frac{J_{\text{ext}}}{J_{\text{dem}}}\varepsilon_p^{v_{\text{dem}}}}{\varepsilon_p^{v_{\text{dem}}} + \frac{J_{\text{cat}}}{J_{\text{dem}}}\varepsilon_p^{v_{\text{cat}}} - \frac{J_{\text{bio}}}{J_{\text{dem}}}\varepsilon_p^{v_{\text{bio}}} - \frac{J_{\text{ext}}}{J_{\text{dem}}}\varepsilon_p^{v_{\text{ext}}}} \tag{2.7}$$

$$C_{\text{cat}}^{J_{\text{dem}}} = \frac{-\frac{J_{\text{cat}}}{J_{\text{dem}}}\varepsilon_p^{v_{\text{dem}}}}{\varepsilon_p^{v_{\text{dem}}} + \frac{J_{\text{cat}}}{J_{\text{dem}}}\varepsilon_p^{v_{\text{cat}}} - \frac{J_{\text{bio}}}{J_{\text{dem}}}\varepsilon_p^{v_{\text{bio}}} - \frac{J_{\text{ext}}}{J_{\text{dem}}}\varepsilon_p^{v_{\text{ext}}}} \tag{2.8}$$

$$C_{\text{dem}}^{J_{\text{dem}}} = \frac{\frac{J_{\text{cat}}}{J_{\text{dem}}}\varepsilon_p^{v_{\text{cat}}} - \frac{J_{\text{bio}}}{J_{\text{dem}}}\varepsilon_p^{v_{\text{bio}}} - \frac{J_{\text{ext}}}{J_{\text{dem}}}\varepsilon_p^{v_{\text{ext}}}}{\varepsilon_p^{v_{\text{dem}}} + \frac{J_{\text{cat}}}{J_{\text{dem}}}\varepsilon_p^{v_{\text{cat}}} - \frac{J_{\text{bio}}}{J_{\text{dem}}}\varepsilon_p^{v_{\text{bio}}} - \frac{J_{\text{ext}}}{J_{\text{dem}}}\varepsilon_p^{v_{\text{ext}}}} \tag{2.9}$$

The flux summation theorem [1] states that the four J_{dem}-control coefficients must sum to one, i.e., the sum of the numerators must equal the denominator. Using the steady-state flux-relationship

$$J_{\text{dem}} = J_{\text{bio}} + J_{\text{ext}} - J_{\text{cat}} \tag{2.10}$$

and therefore,

$$\frac{J_{\text{bio}}}{J_{\text{dem}}} + \frac{J_{\text{ext}}}{J_{\text{dem}}} - \frac{J_{\text{cat}}}{J_{\text{dem}}} = 1 \tag{2.11}$$

this can be seen to be true.

From eqn. 2.9 the following condition ensures a high degree of J_{dem}-control by demand, i.e., $C_{\text{dem}}^{J_{\text{dem}}} \to 1$:

$$\varepsilon_p^{v_{\text{dem}}} \ll \frac{J_{\text{cat}}}{J_{\text{dem}}}\varepsilon_p^{v_{\text{cat}}} - \frac{J_{\text{bio}}}{J_{\text{dem}}}\varepsilon_p^{v_{\text{bio}}} - \frac{J_{\text{ext}}}{J_{\text{dem}}}\varepsilon_p^{v_{\text{ext}}} \tag{2.12}$$

Usually, $\varepsilon_p^{v_{\text{bio}}}$ and $\varepsilon_p^{v_{\text{ext}}}$ are negative quantities (P is the product of the biosynthetic and external supply blocks; increasing p inhibits the fluxes through these blocks). In terms of absolute values the above condition is:

$$\varepsilon_p^{v_{\text{dem}}} \ll \frac{J_{\text{cat}}}{J_{\text{dem}}}\varepsilon_p^{v_{\text{cat}}} + \frac{J_{\text{bio}}}{J_{\text{dem}}}|\varepsilon_p^{v_{\text{bio}}}| + \frac{J_{\text{ext}}}{J_{\text{dem}}}|\varepsilon_p^{v_{\text{ext}}}| \tag{2.13}$$

It should also be clear that if this condition holds the collective control of the other three blocks over the demand flux approaches zero.

The condition for J_{dem}-control by demand is rather complex, depending not only on the relative values of elasticity coefficients, but also on the flux-distribution in the system. So, for example, despite $\varepsilon_p^{v_{\text{bio}}}$ being large, $\frac{J_{\text{bio}}}{J_{\text{dem}}}\varepsilon_p^{v_{\text{bio}}}$ can be small because $\frac{J_{\text{bio}}}{J_{\text{dem}}}$ is small. In a general analysis of this condition one would have to weigh and compare many factors. However, we are designing and not analysing, so what we are looking for is a sufficient condition for J_{dem}-control by demand in a range of demand-flux values: it should be clear that if $\varepsilon_p^{v_{\text{dem}}} \to 0$, then demand will control the flux at any finite value of the right-hand sum in eqn. 2.12.

As in the previous section, our view of the system is simplified considerably if we consider the system in terms of only two blocks: the internal rate with rate v_{dem} and a combined 'supply' with rate $v_{\text{sup}} = v_{\text{bio}} + v_{\text{ext}} - v_{\text{cat}}$ (we use the word 'supply' even though it contains the catabolic branch, which, strictly speaking, is a demand for P). The elasticity of this combined supply with respect to p can be written as the weighted sum of individual elasticities

$$\varepsilon_p^{v_{\text{sup}}} = \frac{J_{\text{cat}}}{J_{\text{dem}}}\varepsilon_p^{v_{\text{cat}}} - \frac{J_{\text{bio}}}{J_{\text{dem}}}\varepsilon_p^{v_{\text{bio}}} - \frac{J_{\text{ext}}}{J_{\text{dem}}}\varepsilon_p^{v_{\text{ext}}} \tag{2.14}$$

This is the same as the right-hand sum in eqn. 2.12, so that the expressions for the flux-control coefficients for the supply and demand blocks reduce to those given in eqns. 2.1 and 2.2.

2.3 Rate characteristics as a design tool

In the previous section we used rate characteristics for visualising a steady state and the response to perturbations around that steady state. We used log-log rate characteristics because the tangential slopes are the scaled elasticity coefficients. Although control analysis is usually based on scaled elasticity coefficients, it is possible to cast the control analytic equations in terms of unscaled (or even half-scaled) coefficients and use unscaled (or half-scaled, i.e., semi-log) rate characteristics.

If the only purpose of the rate characteristic is to consider a single steady state, any one of these rate characteristic formats would do. However, as soon as one wants to compare the responses at two different steady states, then, as argued by Hofmeyr [9], only scaled coefficients and the log-log form of the rate characteristic will suffice. The debate whether we should use scaled or unscaled control coefficients goes back a long way. Purely in terms of mathematics scaling is unnecessary, and a number of theoretical papers, the

one by Reder [18] being a prime example, have used unscaled control and elasticity coefficients. The original reason for using scaled coefficients was that, whereas the value of an absolute change depends on the dimensions, a relative change is dimensionless [1]. The question, however, is why the prevailing steady-state, which changes, instead of an unvarying standard state should be used to get rid of the dimensions. Hofmeyr [9], argued that in most circumstances we want to compare changes in state, rather than the states themselves, and a particular change can have very different effects in different contexts. For example, an absolute flux change from 10 to 11 μM/min represents a 10% change, whereas the same absolute change from 100 to 101 μM/min represents only a 1% change. If we had scaled these changes to a standard state we may have eliminated the units, but not the problem caused by comparing changes at different steady state points on the rate scale. Hofmeyr [9] illustrated his reasoning with rate characteristics and parameter portraits, clearly showing how misleading unscaled plots can be. To sum up, logarithmic scales have the advantage over linear scales that equal distances on any part of the log scale are equivalent to equal percentage changes.

When analysing branched systems such as the 4-way junction the situation is somewhat more complicated. The elasticities in the expressions for scaled control coefficients (which we have just argued to be the ones we should consider) are multiplied with a flux: a re-arrangement of, for example, eqn. 2.6 shows this clearly:

$$C_{\text{bio}}^{J_{\text{dem}}} = \frac{J_{\text{bio}}\varepsilon_p^{v_{\text{dem}}}}{J_{\text{dem}}\varepsilon_p^{v_{\text{dem}}} - J_{\text{bio}}\varepsilon_p^{v_{\text{bio}}} - J_{\text{ext}}\varepsilon_p^{v_{\text{ext}}} + J_{\text{cat}}\varepsilon_p^{v_{\text{cat}}}} \tag{2.15}$$

The question is whether it is possible to construct a rate characteristic where the slopes of the rate curves directly correspond to these flux-elasticity products. For the product in the denominator this is certainly possible: each particular flux actually unscales the $\partial \ln v = \frac{\partial v}{v}$ part of each elasticity since in steady state the rate is equal to the flux. For example, $J_{\text{dem}}\varepsilon_p^{v_{\text{dem}}} = \frac{\partial v_{\text{dem}}}{\partial \ln p}$. This means that a graph of v against $\ln p$ has the required property (Fig. 2.5 b). However, the numerator of the control coefficient does not simplify in this way. When written in half-scaled form, it becomes multiplied by a flux ratio. For example,

$$J_{\text{bio}}\varepsilon_p^{v_{\text{dem}}} = \frac{J_{\text{bio}}}{J_{\text{dem}}} J_{\text{dem}}\varepsilon_p^{v_{\text{dem}}} = \frac{J_{\text{bio}}}{J_{\text{dem}}} \frac{\partial v_{\text{dem}}}{\partial \ln p} \tag{2.16}$$

The slope of half-scaled rate characteristics and flux-ratios therefore determine relative (percentage) control. Unscaled rate characteristics (Fig. 2.5 a) do not suffer from this deficiency because the expressions for unscaled coefficients in terms of unscaled elasticities do not contain explicit fluxes. For example,

$$\tilde{C}_{\text{bio}}^{J_{\text{dem}}} = \frac{\tilde{\varepsilon}_p^{dem}}{\tilde{\varepsilon}_p^{v_{\text{dem}}} - \tilde{\varepsilon}_p^{v_{\text{bio}}} - \tilde{\varepsilon}_p^{v_{\text{ext}}} + \tilde{\varepsilon}_p^{v_{\text{cat}}}} \tag{2.17}$$

where the tilde denotes unscaled coefficients, i.e., $\tilde{C}_{\text{bio}}^{J_{\text{dem}}} = \frac{dJ_{\text{dem}}}{dv_{\text{bio}}}$ and $\tilde{\varepsilon}_x^v = \frac{\partial v}{\partial x}$. However, as explained above, we want to avoid using unscaled control coefficients.

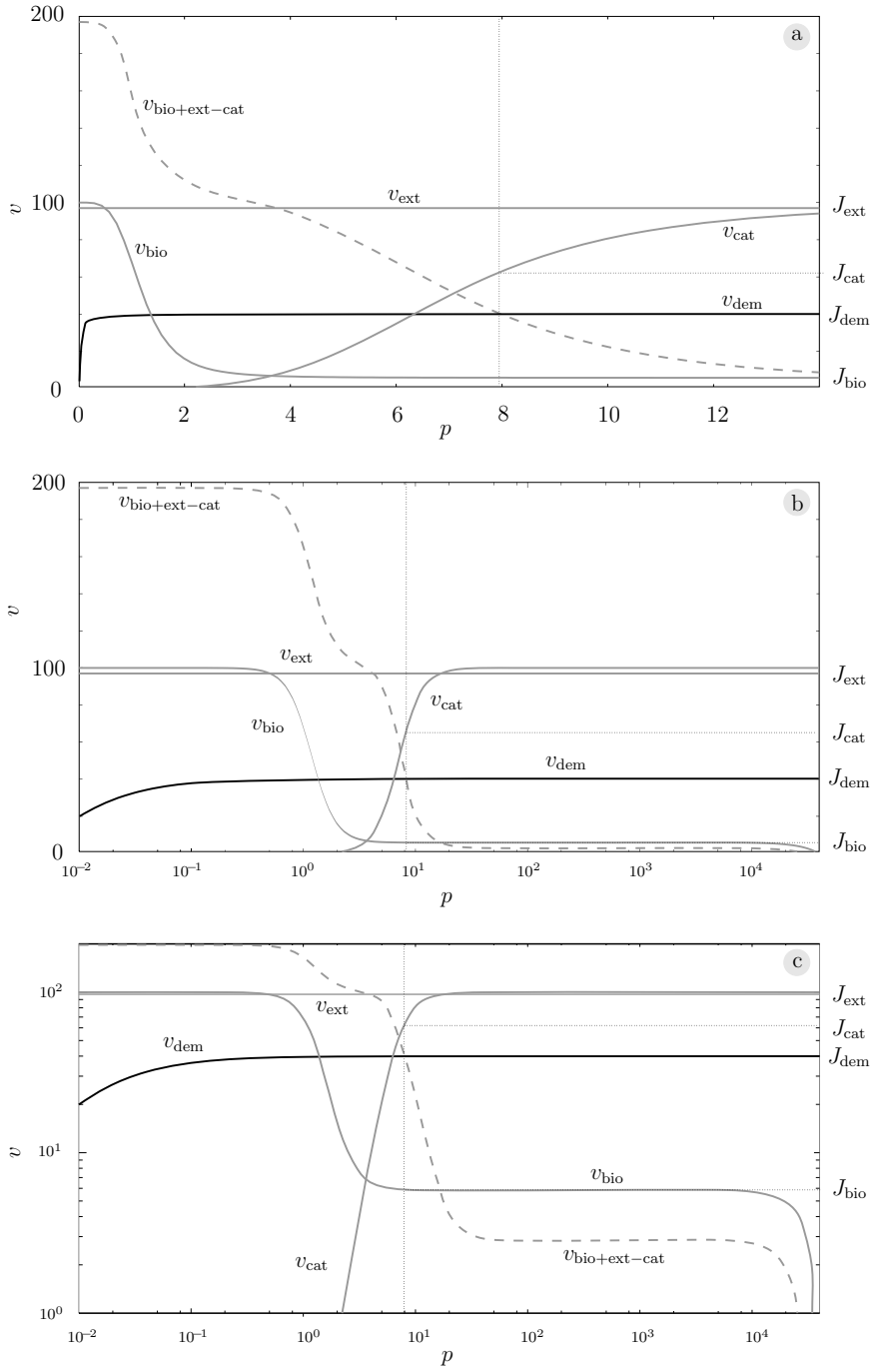

Fig. 2.5 *Different formats of rate characteristics of the 4-way junction.* a Unscaled; b Half-scaled (semi-log); c Fully scaled (log-log). The dashed curve represents the sum $v_{\text{bio}} + v_{\text{ext}} - v_{\text{cat}}$; the steady state obtains where this curve intersects with v_{dem}. The four steady-state fluxes can be read off at the intersection of the rate curves with the vertical line through the steady-state point as shown on the graph.

Whether we use half-scaled or fully scaled elasticity coefficients (and, therefore, semi-log or log-log rate characteristics), we cannot escape from also considering fluxes or flux-ratios when we analyse control. We therefore continue to use log-log rate characteristics (Fig. 2.5 c) and fully scaled elasticity coefficients, which both have additional advantages.

Log-log rate characteristics can show the behaviour of the system over large ranges of both flux and concentration; because equal distances on any part of the scale are equivalent to equal percentage changes, such a graph gives a panoramic view of the relative behaviour of the system. When one compares Fig. 2.5 c with a and b, it is clear that only the fully scaled graph can show both the behaviour near and far from equilibrium and at very low and very high demand. Although the half-scaled graph does depict the full concentration range, it obscures the rapid rate descent at near equilibrium concentrations of P, which in the fully scaled graph leads to a clear homeostatic profile, comparable to a similar homeostatic range around a far-from-equilibrium p of 1. The algebraic expressions for fully scaled elasticity coefficients derived from rate equations are also much simpler than and easier to interpret than those of half-scaled or unscaled elasticities.

3 Moulding the supply rate characteristic: from thermodynamic to kinetic regulation

3.1 Creating a benchmark system

In order to design a biosynthetic supply successfully we first need to establish a basic system which can serve as benchmark for the performance of future designs. We assume the supply block to consist of three reactions that convert S to P via intermediates A and B. In designing this block we can in principle change anything kinetic, but we shall assume that we cannot change thermodynamic properties such as the equilibrium constants, even though, as will be discussed below, Nature is less severely limited in this respect.

The first thing to do is therefore to consider the thermodynamics of the system, i.e., the equilibrium constants of the individual reactions. Because we are not considering a particular 'real' system where the K_{eq}-values have been experimentally determined, we have to assign these values ourselves to begin with and from then on consider them immutable. We could start off by just setting them all to one. However, the main reason for not doing this is that it would mean equal equilibrium concentrations for all intermediates, which would be difficult to distinguish on a graph. We compromised by setting the equilibrium constant K_1 to 400, and K_2 and K_3 to 10. When s is clamped at a concentration of 1, this leads to equilibrium values of 400, 4000, and 40000 for A, B, and P respectively and thereby sets the upper limits of the ranges within which the intermediates can move.

In 'real life' systems the first reaction in a sequence often has a large equilibrium constant compared to the rest of the reactions. That is why we decided to assign the first reaction a relatively large K_{eq}; this choice of value, however, is arbitrary. Nevertheless, once we have made the choice we must live with it. Nature is, of course, less limited: it can for example create a new reaction by coupling it to phosphorylation by ATP, i.e., if $\text{S} \rightleftharpoons \text{A}$ becomes $\text{S} + \text{ATP} \rightleftharpoons \text{A} + \text{ADP} + \text{P}_\text{i}$ the equilibrium ratio a/s can be changed by a factor of 10^8 at the prevailing steady-state values of ATP, ADP, and P_i [13]. Another way in which a high equilibrium ratio a/s can be maintained, even if the equilibrium constant is small, is if the reaction depends on a pair of cofactors that are clamped at a opposing ratio. For example, if the reaction $\text{S} + \text{NAD} \rightleftharpoons \text{A} + \text{NADH}$ has an equilibrium

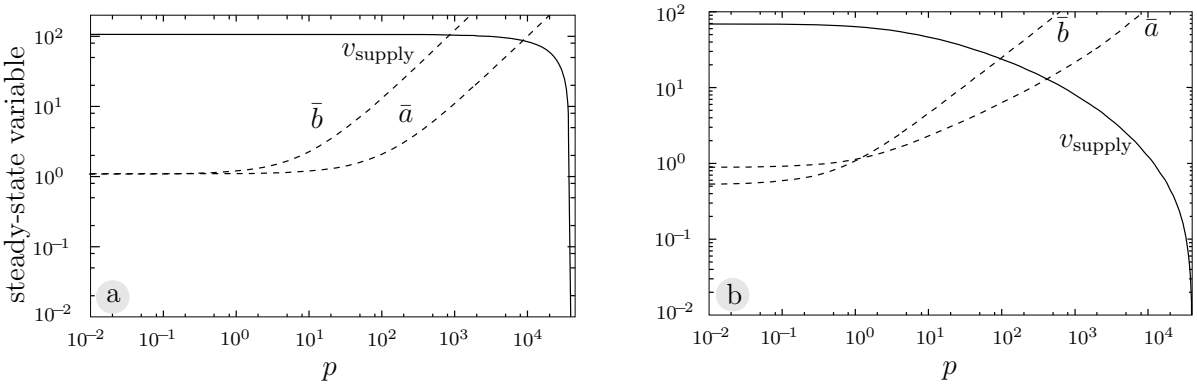

Fig. 3.1 *Mass-action versus Michaelis-Menten kinetics.* a All reactions have the rate equation $v = 100(x - \frac{y}{K_{\text{eq}}})$ with equilibrium constants of reactions 1, 2 and 3 set to 400, 10, and 10. b Reactions have the kinetics shown in Fig. 3.2 with the uncompetitive dissociation constant of E_3 $K_{\text{iu}} \to \infty$ and the competitive dissociation constant $K_{\text{ic}} = 1$.

constant of 1, the equilibrium ratio of a/s can be set to 10^4 if NADH/NAD ratio is maintained at 10^{-4} by other reactions in the cell. In general, Nature has some freedom to decide which reactions to use and the order in which to them in. In recent years a number of interesting studies have addressed this topic [19, 20, 21, 22, 23, 24, 25, 26]

Now turning to kinetics, we start off with 'what inanimate nature has given us' as a benchmark, i.e., we assign each reaction the reversible mass-action rate equation $v = 100(x - \frac{y}{K_{\text{eq}}})$, where the rate constant value of 100 sets a suitable rate range. The supply steady state is then calculated for a range of p from 0 to its equilibrium concentration of 40000 (the curves in Fig. 3.1 a).

Mass-action clearly does not enable the flux to respond to p except when approaching equilibrium, where the flux decreases steeply. This can be regarded as pure *thermodynamic regulation*. Although this situation satisfies the design criterion that requires a steep decrease of supply flux over a narrow percentage band of p, it does so at near-equilibrium a, b, and p. In general, overall equilibrium constants of pathways can be quite high, leading to high concentrations near equilibrium that could exhaust the solvent capacity of the cell and could become toxic [13]. We want to design against this property: supply flux should decrease over a narrow percentage band of p at low concentrations *far from equilibrium*. Like living cells, we now add enzymes to try and change the behaviour of the supply. Enzymes speed up the reactions and, by binding substrates and products, change the kinetic order of the reactions (the elasticities). Although the flux through the enzyme-catalysed supply should be much higher than that through the mass-action system we assume, for the sake of comparison, that we will be working on identical rate scales.

3.2 A vanilla Michaelis-Menten system

We would like to start with a functionally undifferentiated system that we can mould into the required shape. All three reactions are therefore regarded as catalysed by simple reversible Michaelis-Menten enzymes, so that each reaction is subject at least to competitive product inhibition (see Fig. 3.2). We initially set the values of s and all K_m-values to 1 (see figure legend for E_3 parameter settings). The limiting rates determine the rate scale and therefore the catalytic capacity of the biosynthetic system; we set all three to 200. Because s/K_s of E_1 is 1 this means that the limiting rate of the biosynthetic block is 100, which gives a convenient rate scale to work with.

$$v_1 = \frac{200\left(s - \frac{a}{400}\right)}{1+s+a} \qquad v_2 = \frac{200\left(a - \frac{b}{10}\right)}{1+a+b} \qquad v_3 = \frac{200\left(b - \frac{p}{10}\right)}{1 + b\left(1 + \frac{p}{K_\mathrm{iu}}\right) + \frac{p}{K_\mathrm{ic}}} \qquad v_\mathrm{dem} = \frac{V_\mathrm{dem}\, p}{0.001 + p}$$

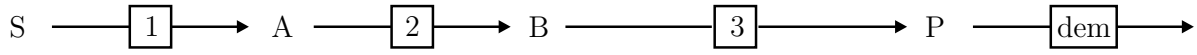

Fig. 3.2 *A 3-step supply block.* The rate equations are instances of the general equation $v = \frac{V_\mathrm{f}}{K_\mathrm{s}}\left(s - \frac{p}{K_\mathrm{eq}}\right) / \left(1 + \frac{s}{K_\mathrm{s}} + \frac{p}{K_\mathrm{p}}\right)$. The concentration of S is clamped at its $s_{0.5}$-value of 1. For all reactions K_s and K_p are set to 1 and therefore have been omitted from the rate equations. The exception is the rate equation for E_3 which allows for mixed inhibition by its immediate product P. When the uncompetitive dissociation constant $K_\mathrm{iu} \to \infty$ and the competitive dissociation constant $K_\mathrm{ic} = 1$, the reaction has the same kinetics as the others. When $K_\mathrm{ic} \to \infty$ and $K_\mathrm{iu} = 1$, E_3 is uncompetitively inhibited by P.

The way that this Michaelis-Menten system responds to the full range of p variation is shown in Fig. 3.1 b. Compared to the sharp decrease in flux at near-equilibrium shown by the mass-action system, the Michaelis-Menten system gives a gradual decrease in flux over a 40 000-fold change in p. The flux is considerably more sensitive to lower values of p than it is with mass action and steadily decreases from $p \approx 1$ upwards. This is clearly a kinetic effect: thermodynamic regulation takes over only at very high p. However, it still takes approximately a 10^4-fold change from $p \approx 1$ to give a 100-fold change in flux. This behaviour does not, therefore, satisfy our design criterion related to flux regulation. If we now examine the behaviour of the internal metabolites A and B in Fig. 3.1 a, it is clear that they even when p is still quite far from equilibrium, a and b already start tracking P at a near-equilibrium ratio. The situation is slightly better in the enzyme-catalysed system in Fig. 3.1 b. We are now, however, primarily interested in the flux profile of the system and we could conceivably improve the situation by increasing the affinity of each enzyme for its immediate product as shown in Fig. 3.3.

The graph in a shows the response of the flux to increased product binding. Clearly, the product inhibition effect increases, but the profile is 'flattened out' over a large range of product concentration until it is almost a straight line. Over this p-range the flux-carrying capacity is also decreased. Both of these effects contradict our design principles

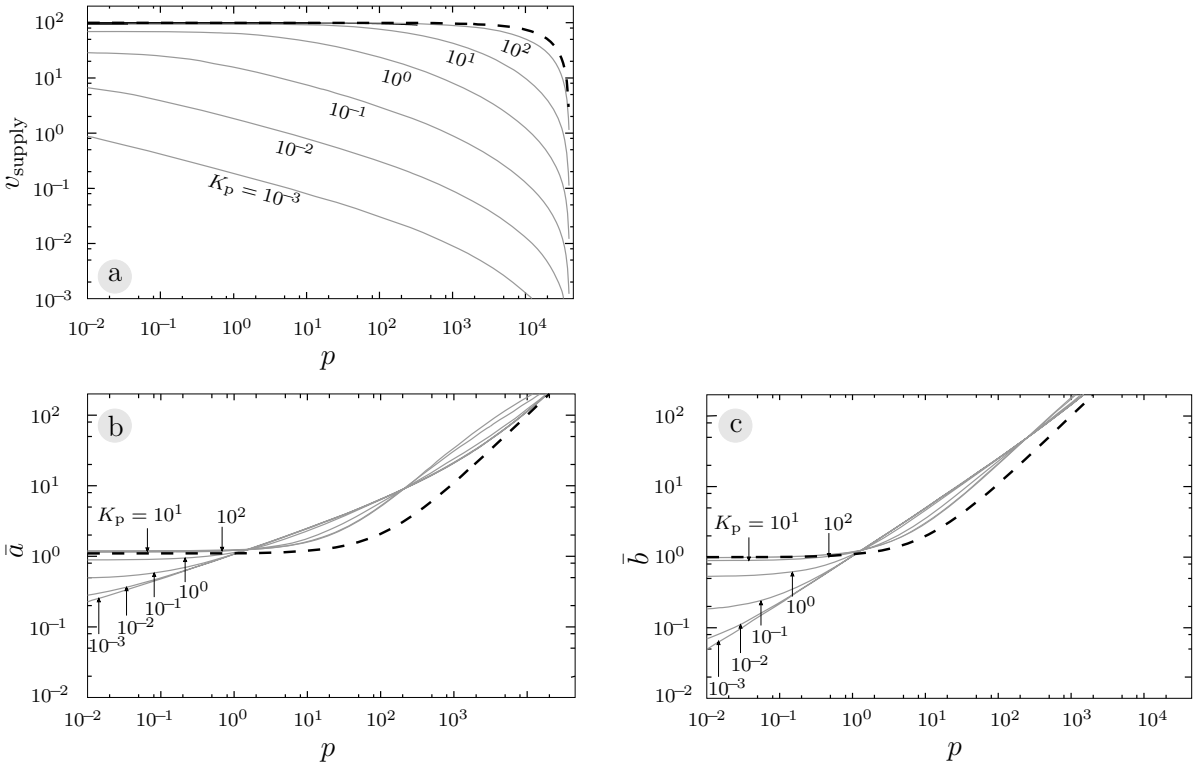

Fig. 3.3 *Increasing the affinity of all the enzymes for their product.* (a) The effect on the flux of simultaneously changing the K_{p}-values of E_1, E_2, and E_3 (always to equal values). (b) The effect on $\bar{a}$. (c) The effect on $\bar{b}$. The dashed line is the benchmark mass-action behaviour from Fig. 3.1(a).

and should definitely be avoided. Fig. 3.3 b and c show the metabolite profiles, which also flatten out as the strength of product binding increases.

In the next section we examine the possibilities opened up by other types of direct product inhibition for moulding the behaviour of the system in the desired direction. However, instead of changing the properties of all three biosynthetic enzymes as above, we would like to achieve the desired profile by tinkering with one enzyme only. In the next section we use control analysis to find the best candidate.

3.3 Competitive versus uncompetitive product inhibition

A control analysis of the biosynthetic supply system helps us understand the factors that determine the flux-response to p [27]. The slope of the rate characteristic (the elasticity of supply with respect to p) can be written as a partitioned response [1]:

$$\varepsilon_p^{v_{\text{supply}}} = C_3^{J_{\text{supply}}} \varepsilon_p^{v_3} = \frac{\varepsilon_a^{v_1} \varepsilon_b^{v_2}}{\varepsilon_a^{v_2} \varepsilon_b^{v_3} - \varepsilon_a^{v_1} \varepsilon_b^{v_3} + \varepsilon_a^{v_1} \varepsilon_b^{v_2}} \varepsilon_p^{v_3} \tag{3.1}$$

A sufficient condition for $C_3^{J_{\text{supply}}}$ to approach its maximum of 1 is that $\varepsilon_b^{v_3} \to 0$. Combined with a high $\varepsilon_p^{v_3}$ this condition should ensure a strong inhibitory response of J_{supply} to p.

From classical enzyme kinetics we know that the basic forms of reversible inhibition are all instances on the scale from pure competitive to pure uncompetitive inhibition [8]. To start off we simulated the biosynthetic subsystem as defined in Fig. 3.2 at these two extremes (see Fig. 3.4).

The graphs show how the supply flux and intermediate concentrations respond to p at increasing strengths of inhibition (decreasing inhibition constants). Clearly, uncompetitive inhibition is a more effective inhibitory mechanism than competitive inhibition in that the slope of the uncompetitively inhibited rate curve (the elasticity coefficient $\varepsilon_p^{v_{\text{supply}}}$) is 1 above $p \approx 1$, whereas that of the competitively inhibited rate curve is always much less than 1. However, a price for this increase in flux-sensitivity is that intermediates A and B build up to near-equilibrium values at much lower levels of p (compare c and e with d and f).

What is the basis for this difference in response profiles? The maximum value of $\varepsilon_p^{v_{\text{supply}}}$ depends on $\varepsilon_p^{v_3}$, which, for the reversible Michaelis-Menten mechanism, reaches a maximum of -1, irrespective of the type of inhibition. Concomitantly, as shown above, $\varepsilon_b^{v_3}$ should be as small as possible to ensure effective J_{supply}-control by E_3. Uncompetitive inhibition is the only mechanism that ensures a decrease in $\varepsilon_b^{v_3}$ with an increase in p, while competitive inhibition forces a concomitant increase in $\varepsilon_b^{v_3}$ [27]. This is clear from

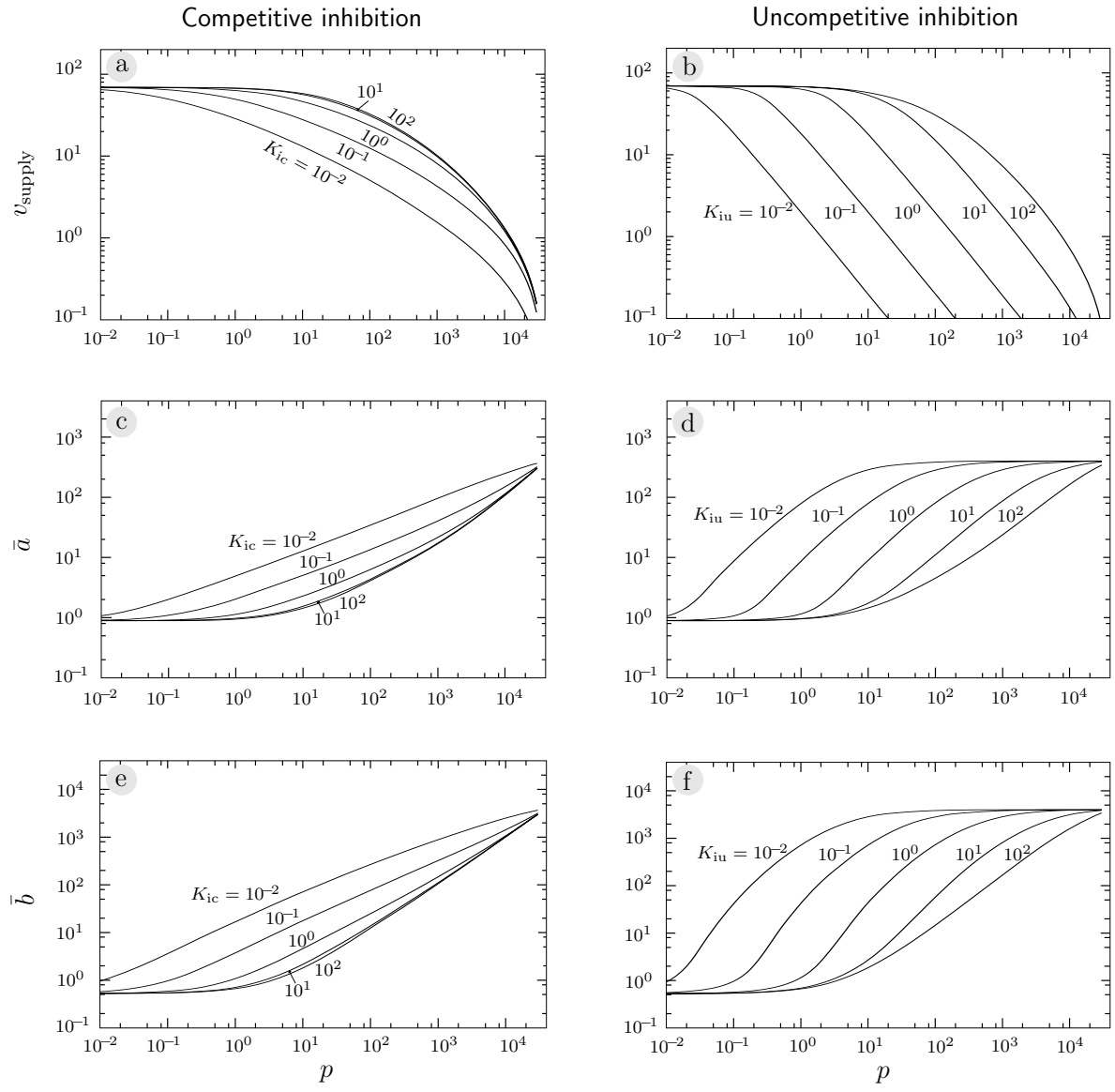

Fig. 3.4 *The effect of competitive versus uncompetitive inhibition of* E_3 *by* P *on the steady-state variables of the biosynthetic supply.* In a, c, and e we vary the strength of competitive inhibition in the absence of uncompetitive inhibition ($K_{\mathrm{iu}} = 10^{12}$), while in b, d, and f we vary the uncompetitive inhibition in the absence of competitive inhibition ($K_{\mathrm{ic}} = 10^{12}$).

the expression that describes how the elasticity $\varepsilon_b^{v_3}$ varies with p [27]:

$$\frac{\partial \ln \varepsilon_b^{v_3}}{\partial \ln p} = \frac{\dfrac{b}{K_\mathrm{b}}\dfrac{p}{K_\mathrm{iu}}\left(\dfrac{K_\mathrm{iu}}{K_\mathrm{ic}} - 1\right)}{\left(1 + \dfrac{p}{K_\mathrm{ic}}\right)\left(1 + \dfrac{b}{K_\mathrm{b}}\left(1 + \dfrac{p}{K_\mathrm{iu}}\right) + \dfrac{p}{K_\mathrm{ic}}\right)} \tag{3.2}$$

The numerator term $\frac{K_\mathrm{iu}}{K_\mathrm{ic}} - 1$ determines how $\varepsilon_b^{v_3}$ depends on p. Only when $K_\mathrm{iu} < K_\mathrm{ic}$, i.e., when the uncompetitive component dominates the competitive component, is an increase in p necessarily accompanied by a decrease in $\varepsilon_b^{v_3}$. If inhibition by p is purely uncompetitive ($K_\mathrm{ic} \to \infty$), its decreasing effect on $\varepsilon_b^{v_3}$ is maximal. When the competitive component dominates, $\varepsilon_b^{v_3}$ necessarily increases. With noncompetitive inhibition (when $K_\mathrm{iu} = K_\mathrm{ic}$), changes in p do not affect $\varepsilon_b^{v_3}$ so that the substrate and product elasticities are uncoupled.

The crucial quantities in understanding the flux-control profiles of the different types of inhibition are $C_3^{J_\mathrm{supply}}$, $\varepsilon_b^{v_3}$ and $\varepsilon_p^{v_3}$. Their variation with p are shown in Fig. 3.5, which again compares the two types of inhibition. Note how in the uncompetitive case $C_3^{J_\mathrm{supply}}$ increases to 1 as $\varepsilon_b^{v_3}$ decreases to zero, while $\varepsilon_p^{v_3}$ concomitantly becomes more negative, approaching -1. As the strength of uncompetitive inhibition decreases the effect weakens; at high values of K_iu the profile changes dramatically. As discussed in Section 1.3 elasticity coefficients can always be dissected into a thermodynamic and a kinetic part [9]. The thermodynamic part can be calculated as $1/(1-\rho)$ for substrates and $-\rho/(1-\rho)$ for products, where ρ is the disequilibrium ratio Γ/K_eq with Γ the mass-action ratio. The uncompetitive inhibition profile shifts because the kinetic terms in the $\varepsilon_b^{v_3}$ and $\varepsilon_p^{v_3}$ (which have a ceiling of 1 and -1 respectively) are overwhelmed by the thermodynamic terms, i.e., the systems become thermodynamically regulated, instead of kinetically. In the competitive case the simultaneous and strictly coupled increase in both elasticity coefficients is clearly shown; even with strong product inhibition this mechanism never allows the control coefficient to become high enough for effective flux response to changes in p.

In Fig. 3.6 we provide another view by combining the results for both types of inhibition with an inhibition constant value of 1 on a graph together with the benchmark mass-action profiles.

Fig. 3.6 f also shows the distinction between thermodynamic and kinetic regulatory effects. Near equilibrium, the thermodynamic part (the dashed curve in Fig. 3.6 f) always dominates, while far from equilibrium the kinetic part (the dotted curves) comes into its own.

In terms of feedback by direct product inhibition, uncompetitive inhibition is the best we can do, although it has a drawback in that it forces the system upstream from in the inhibited enzyme to be at the mercy of thermodynamics. Nevertheless, real systems exist where this apparently affords sufficient regulation and where the disadvantage just mentioned is not too great; mammalian serine biosynthesis is a well-studied example [28]. Unless we find kinetic mechanisms that allow $\varepsilon_p^{v_3}$ to exceed -1 we are stuck with a slope of one (while maintaining a near zero $\varepsilon_b^{v_3}$). Also, at high p the upstream section

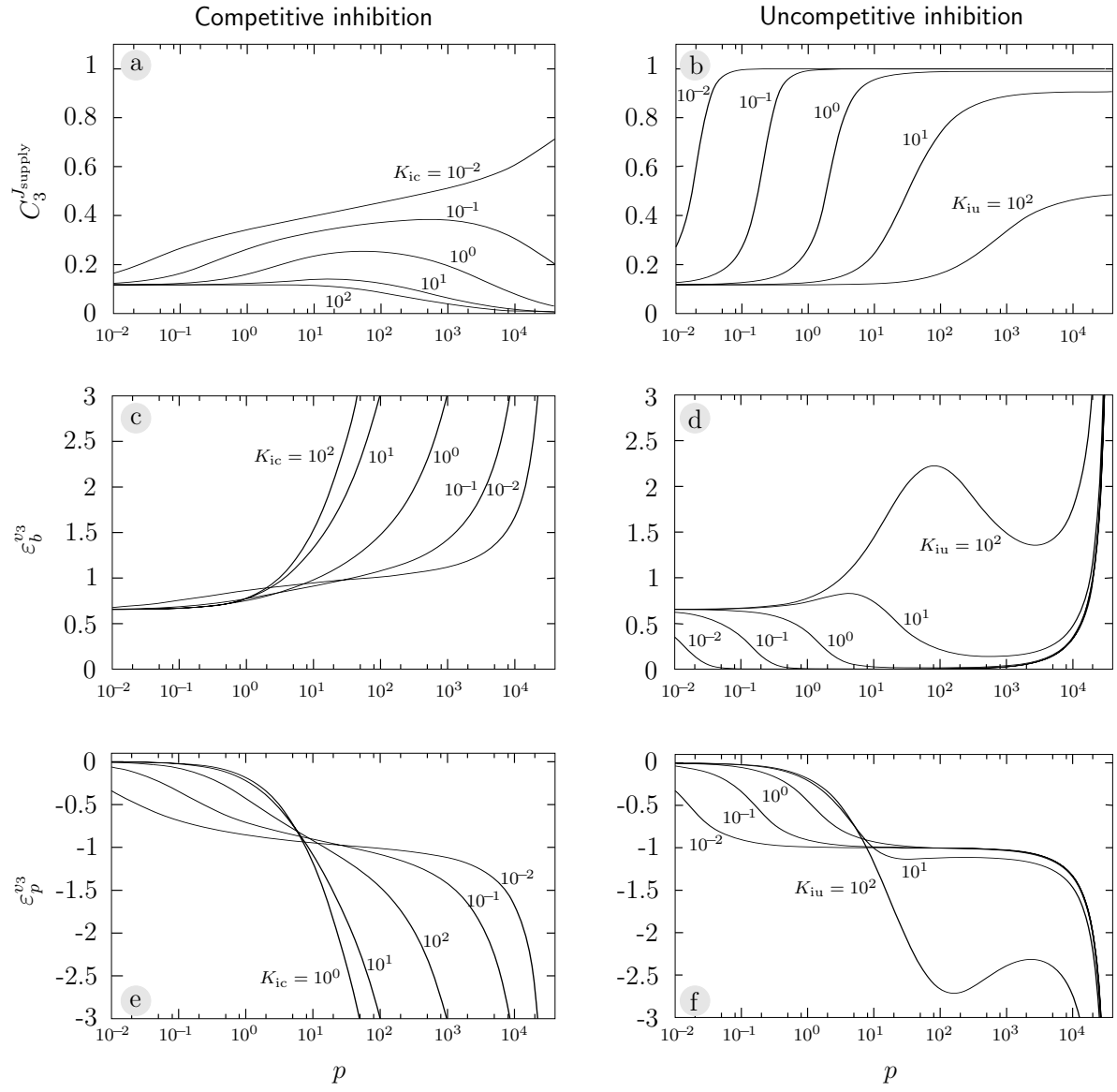

Fig. 3.5 *The effect of competitive versus uncompetitive inhibition of* E_3 *by* P *on the control analysis of the biosynthetic supply.* The parameter values are the same as for Fig. 3.4.

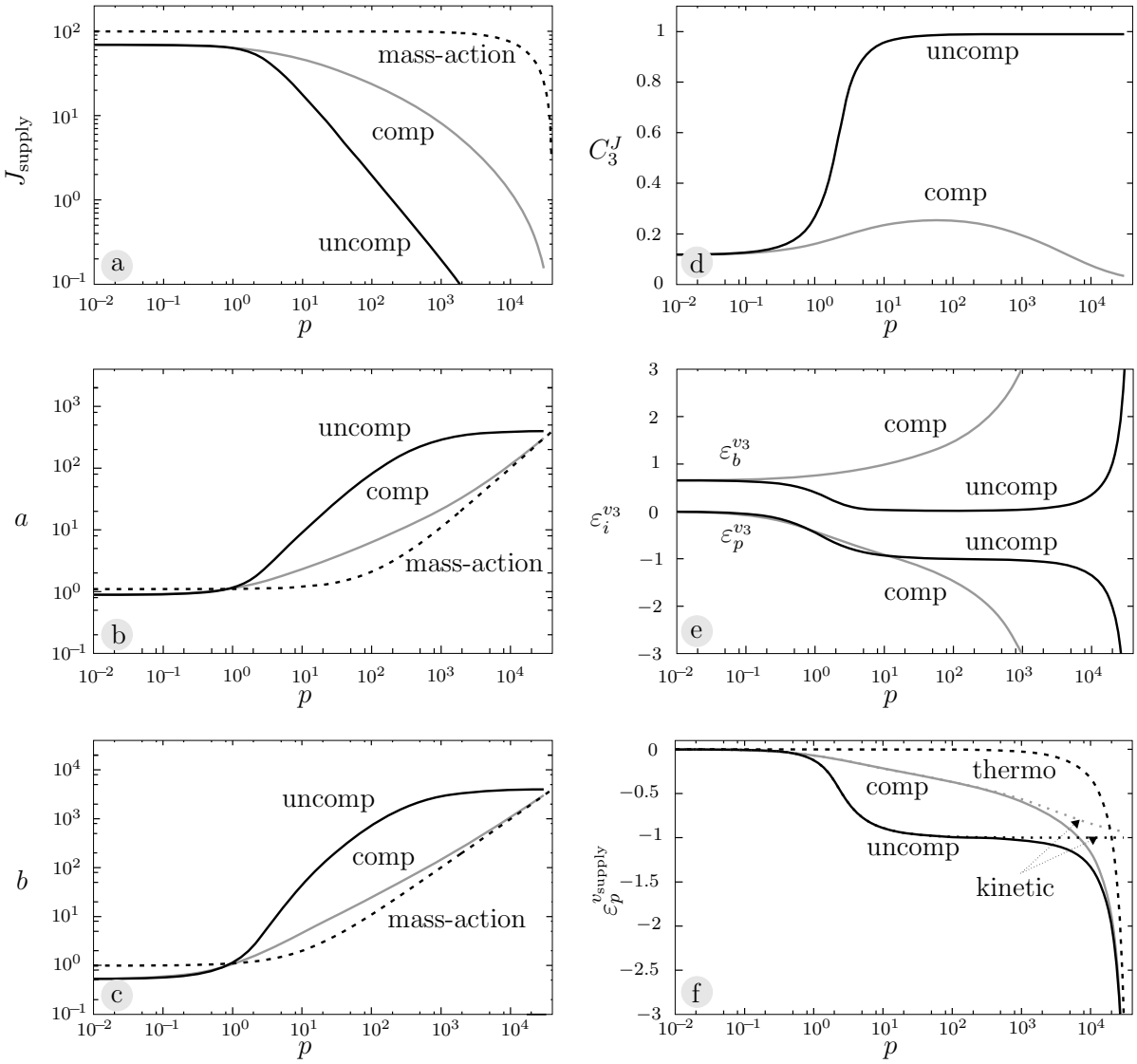

Fig. 3.6 *Kinetic behaviour of the supply system in response to changes in p.* Graphs a, b, and c show how the supply flux and the steady-state concentrations of A and B change for a system with competitive or uncompetitive inhibition of E_3 by P (inhibition constant K_{ic} or K_{iu} of 1 respectively), compared to pure mass-action behaviour. Graphs d, e, and f show how various coefficients change with p; their relevance is discussed in the text.

must tend to equilibrium. Depending on the equilibrium constants, this can mean high intermediate concentrations, and, as we shall show further on, sluggish responses.

3.4 Introducing end-product inhibition of E_1

Ultimately, the problem of any inhibition mechanism that depends on sequential communication up the chain from the inhibited enzyme is that thermodynamics always interferes at some point. The only way to avoid this is to have P communicate directly with the first enzyme in the sequence, E_1. We introduce this direct effect into our system by assigning E_1 either a reversible Michaelis-Menten equation that allows for mixed inhibition by P, or the reversible Hill-rate equation [6], which allows for cooperative effects of S, A, and P, while retaining the reversibility of the reaction. Rate equations and parameter values of the amended system are given in Fig. 3.7.

$$v_1 = \frac{200\left(s - \frac{a}{400}\right)}{1 + \frac{s}{K_\mathrm{s}}\left(1 + \frac{p}{K_\mathrm{iu}}\right) + \frac{a}{K_\mathrm{a}} + \frac{p}{K_\mathrm{ic}}} \qquad v_2 = \frac{200\left(a - \frac{b}{10}\right)}{1 + a + b} \qquad v_3 = \frac{200\left(b - \frac{p}{10}\right)}{1 + b + p} \qquad v_{dem} = \frac{V_\mathrm{f}\, p}{0.001 + p}$$

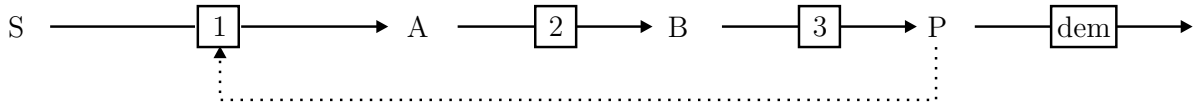

$$v_1 = \frac{\frac{200}{s_{0.5}}\left(s - \frac{a}{400}\right)\left(\frac{s}{s_{0.5}} + \frac{a}{a_{0.5}}\right)^{h-1}}{\left(\frac{s}{s_{0.5}} + \frac{a}{a_{0.5}}\right)^{h} + \frac{1 + \left(\frac{p}{p_{0.5}}\right)^{h}}{1 + \alpha\left(\frac{p}{p_{0.5}}\right)^{h}}}$$

Fig. 3.7 *The same system as in Fig. 3.2 but with* E_1 *subject to end-product inhibition.* The rate of E_1 is described either by the reversible Hill equation with one allosteric modifier [6] or a reversible Michaelis-Menten equation with mixed inhibition by P. The concentration of S is clamped at its $s_{0.5}$-value of 1.

The introduction of a new communication route changes the control analysis of the system. Again we may ask what the basic conditions are under which the supply rate is most sensitive to p. The response of the supply rate to p is now a sum of two communication paths, one up the chain via E_3 as before and one via the feedback onto E_1.

$$\begin{aligned}\varepsilon_p^{v_{\text{supply}}} &= C_3^{J_{\text{supply}}}\varepsilon_p^{v_3} + C_1^{J_{\text{supply}}}\varepsilon_p^{v_1} \\ &= \frac{\varepsilon_a^{v_1}\varepsilon_b^{v_2}}{\varepsilon_a^{v_2}\varepsilon_b^{v_3} - \varepsilon_a^{v_1}\varepsilon_b^{v_3} + \varepsilon_a^{v_1}\varepsilon_b^{v_2}}\varepsilon_p^{v_3} + \frac{\varepsilon_a^{v_2}\varepsilon_b^{v_3}}{\varepsilon_a^{v_2}\varepsilon_b^{v_3} - \varepsilon_a^{v_1}\varepsilon_b^{v_3} + \varepsilon_a^{v_1}\varepsilon_b^{v_2}}\varepsilon_p^{v_1} \qquad (3.3)\end{aligned}$$

How can we ensure that the communication path via E_1 dominates the response to p? If $\varepsilon_a^{v_1} \approx 0$, i.e., if a is far-from-equilibrium and E_1 binds A very weakly, then $C_1^{J_{\text{supply}}} \to 1$, $C_3^{J_{\text{supply}}} \to 0$ and $C_{\text{demand}}^{p} = 1/\varepsilon_p^{v_1}$, i.e., the steady-state p is determined solely by the properties of E_1.

We therefore set either K_a or $a_{0.5}$ of E_1 to a high value of 10^4 (in our simulations the equilibrium ceiling on a at $s = 1$ is 400, which ensures the virtual absence of a kinetic effect of A on E_1 throughout the range of p-variation).

Before introducing cooperativity we compare the three classical inhibition mechanisms (uncompetitive, competitive, and non-competitive) with non-cooperative Hill-kinetics. Kinetically the mechanisms differ as follows:

1. Competitive inhibition: Binding of S, A and P is mutually exclusive; binding of either S, A, or P decreases the apparent K_m of the other two species.

2. Uncompetitive inhibition: P can only bind to the ES or EA-complex and decreases K_s (or K_a) and V_f by the same factor.

3. Non-competitive inhibition: P binds independently from S or A, and does not affect their binding; only V_f is decreased.

4. Hill-inhibition: P binds independently from S or A; binding of P increases $s_{0.5}$ and $a_{0.5}$. P can only affect S or A-binding in a limited range of $s/s_{0.5}$ or $a/a_{0.5}$-values.

Fig. 3.8 shows how supply flux responds to p. The effect of an increasing s/K_s (or $s/s_{0.5}$) was achieved by decreasing K_s (or $s_{0.5}$) at a fixed s of 1. As expected, at low p the flux increases identically with increasing saturation with s for all four situations. At low saturation with s, uncompetitive inhibition by P is much less effective in lowering v_{supply} than competitive inhibition, because there is much less ES-complex to bind to, whereas competitive binding is easier to achieve when s-saturation is low. However, as s-saturation increases, uncompetitive inhibition becomes progressively more effective as the concentration of ES-complex increases, whereas for competitive inhibition it becomes more difficult for P to compete with S. The flux response obtained with non-competitive inhibition is obviously a mixture of uncompetitive and competitive inhibition, in a sense showing the best of both worlds. The non-cooperative Hill effect is the most similar to the competitive effect, but even without cooperativity it shows a unique property that sets it apart from the other mechanisms: the curves are sigmoidal, thereby defining a clear range in which the rate decreases with increasing p before levelling out again (after which it begins the steep descent into equilibrium). It is this property that we hope to exploit to define a narrow range of inhibition far from equilibrium.

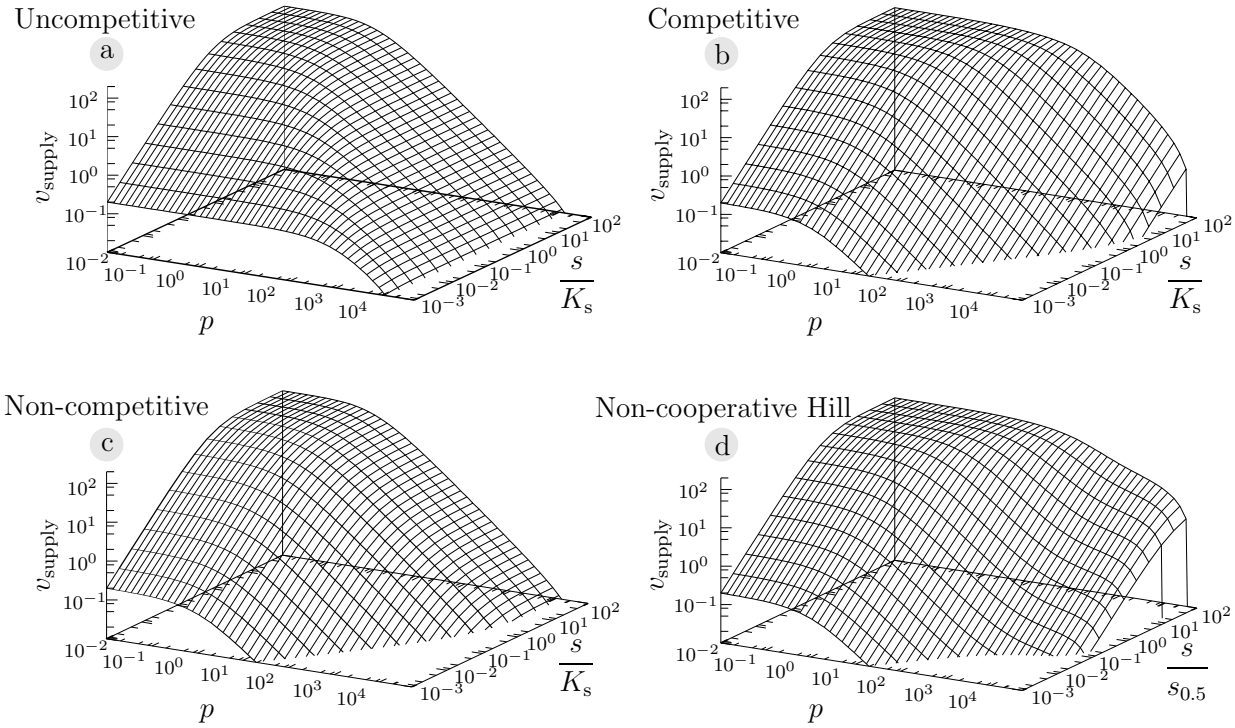

Fig. 3.8 *The effect on flux of four different types of inhibition of the first reaction of the pathway by P.* In a, b, and c E_1 has the rate equation of E_3 in Fig. 3.2, with the following inhibition constants for P: a $K_{\text{ic}} = 10^4$, $K_{\text{iu}} = 1$; b $K_{\text{ic}} = 1$, $K_{\text{iu}} = 10^4$; c $K_{\text{ic}} = 1$, $K_{\text{iu}} = 1$. In d E_1 has the reversible Hill rate equation as in Fig. 3.7 with $h = 1$ and $\alpha = 0.001$.

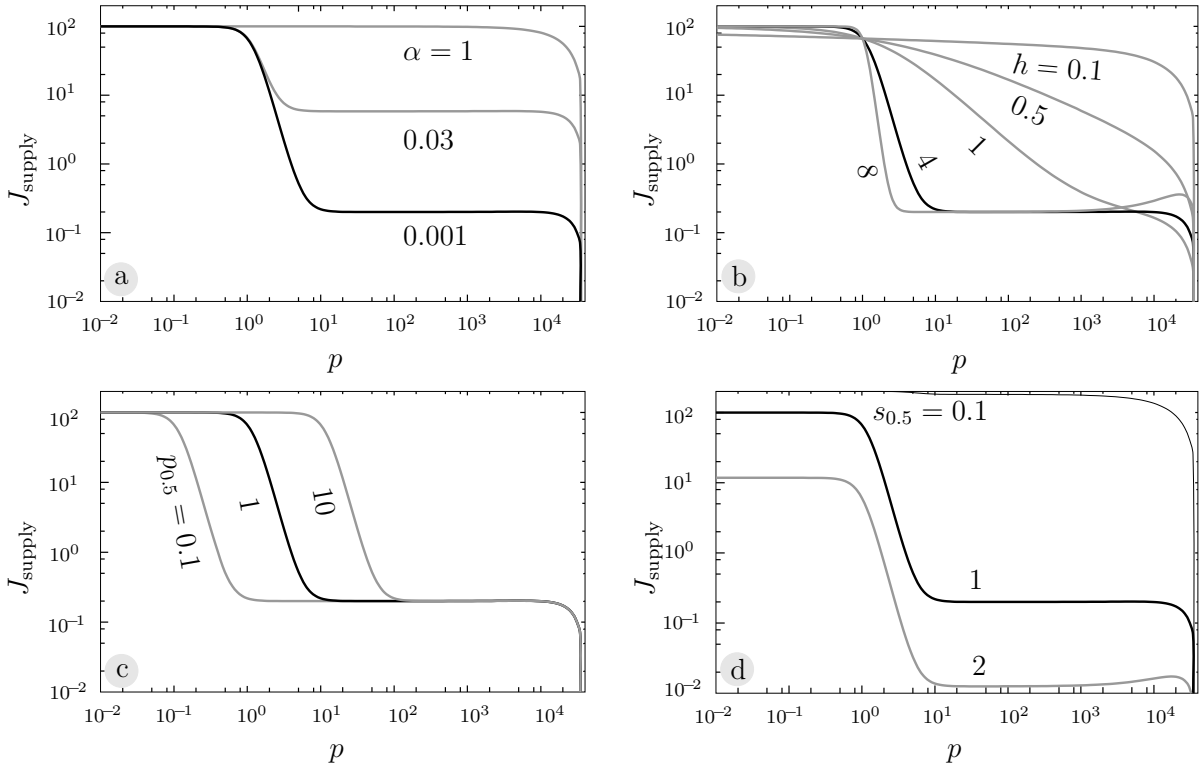

Fig. 3.9 *Tuning the behaviour of supply via the reversible Hill equation.* The effects of the parameters α (graph a), h (graph b), $p_{0.5}$ (graph c), and $s_{0.5}$ (graph d) of this equation (given in Fig. 3.7) are shown when the parameter $a_{0.5}$ is set to 10^4 so that E_1 is kinetically insensitive to its immediate product A. The black reference curve has parameter values of $\alpha = 0.001$, $h = 4$, $s_{0.5} = p_{0.5} = 1$.

3.5 Designing for homeostasis far from equilibrium

We now explore the effect of manipulating the parameters of E_1 with a reversible Hill-mechanism to see whether we can find a set that gives us the desired response of flux to p (Fig. 3.9).

The parameter α determines the strength of inhibition (Fig. 3.9 a), the Hill coefficient h the steepness of the response (Fig. 3.9 b), and the half-effect constant $p_{0.5}$ the range within which P has its inhibitory effect (Fig. 3.9 c). A judicious combination of parameter values transforms the rate characteristic to the desired shape (the black curve in each graph). We demarcate the range in which p operates kinetically by setting the half-effect constant $p_{0.5}$ to 1. This is the closest we can get to the so-called 'set-point' which is so important in the design of technological feedback devices. Next we can make the response around this point steeper by increasing the Hill-coefficient (here to a reasonable value of 4)[1]. The flux-range in which the kinetic effect operates can now be

[1]Note that at an even higher Hill-coefficient of 8 there is an activatory effect of P at high concentrations. The consequences of this interesting phenomenon will be discussed in Chapter 4 where we investigate

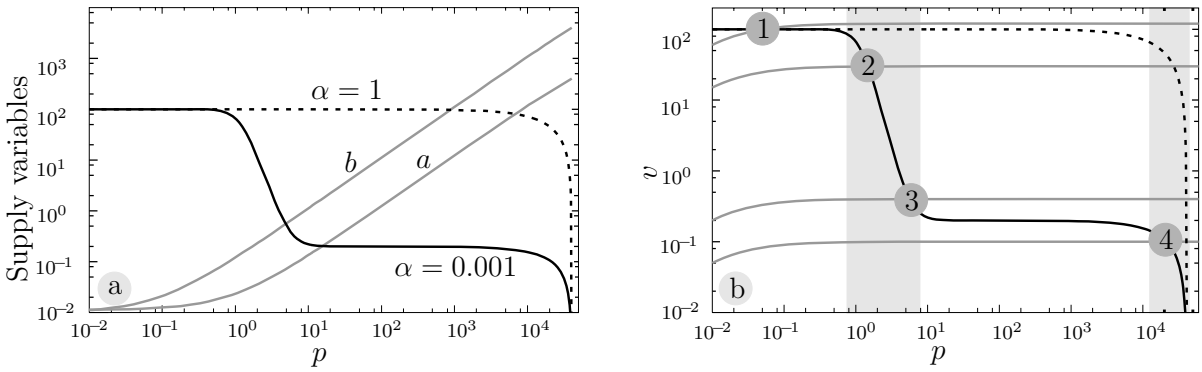

Fig. 3.10 *The steady-state behaviour of biosynthetic supply with and without allosteric end-product inhibition.* Graph a shows the how the biosynthetic flux and the intermediate concentrations a and b respond to the full range of p when enzyme 1 is highly sensitive to P ($\alpha = 0.001$) and when it is desensitised ($\alpha = 1$). Graph b combines these supply characteristics with demand characteristics (with $K_{\text{dem}} = 0.01$) at various values of V_{dem}. The four marked steady states are discussed in the text. The supply rate characteristic has been calculated for parameter values that give the black curve in Fig. 3.9.

adjusted by changing the inhibitory strength factor α. A value of 0.001 allows about a 800-fold flux change between the two plateaus.

It is also clear from Fig. 3.9 d that all the advantages of this type of inhibition are lost at high values of $s/s_{0.5}$. As discussed by Hofmeyr and Cornish-Bowden [6] the reversible Hill-equation and the general Adair-equation (from which it is derived) have the property that they lose their sensitivity to inhibition by allosteric effectors when highly saturated with substrate. In this sense they differs markedly from competitive mechanisms (including the Monod-Wyman-Changeux scheme) where an increase in competitor concentration can always overcome substrate binding, and *vice versa*.

We summarise the effect of allosteric end-product inhibition on the steady-state properties of the biosynthetic supply block in Fig. 3.10 and compare it with a system without end-product inhibition. Fig. 3.10 a shows how the supply variables vary with p when allosteric feedback is present and when E_1 has been desensitised. Fig. 3.10 b combines the supply rate characteristics with those of various demand activities. These graphs make the distinction between kinetic regulation far from equilibrium and thermodynamic regulation near equilibrium particularly clear. The shaded band around steady states 2 and 3 in Fig. 3.10 b shows the range within which p is homeostatically regulated by E_1 at far-from-equilibrium conditions while flux is controlled by demand. However, this regulation has limits: when the demand exceeds the capacity of the supply (steady state 1), the supply takes over control of flux. The regulatory limit can of course be shifted be increasing the limiting reaction velocities of the biosynthetic enzymes. In our system these V_{f}-values are all set to the same value of 200, but usually one finds that the

the effect of increasing the strength with which E_1 binds its immediate product A.

intermediate enzymes (our E_2 and E_3) are much more active than the first, end-product inhibited enzyme (this will be discussed in Chapter 5); when this is true the supply capacity can be adjusted effectively by changing only V_1.

At very low demand a point (steady state 4) is reached where E_1 just cannot keep p sprung far from equilibrium and p jumps onto the thermodynamic arm of the supply rate curve. The shaded band around steady state 4 again shows that even if end-product inhibition is absent, the flux is still controlled by demand activities below the maximum capacity of the supply; $\bar{p}$ is still homeostatic, but only at high near-equilibrium values.

We have reached the point in our story where we have optimised an important part of our design. Our system still responds sensitively to changes in the internal demand within a specified range of variation in product concentration, while we have now also met the following design criterion:

The steady-state concentration of the linking metabolite P (and the other intermediates) should be maintained homeostatically at a low, far-from-equilibrium value. The limited solvent capacity of the cell for its thousands of molecules requires that metabolites do not build up to high concentrations.

Before tackling the question of how rapidly the system responds to changes in demand (where we shall also return to the matter of the intermediate concentrations) and how it behaves in the presence of external supply and catabolism, we take a detour onto an isolated side-road, where we go mushroom-hunting.

4 An isola-ted story of mushroom-induced visions

Up to now we have studied the response of the biosynthetic subsystem to changes in the concentration of its product P by simulating each reaction rate explicitly. It would be very useful if we could capture the steady-state behaviour of the whole biosynthetic system in one rate equation that generates the correct rate characteristic. However, in general such an algebraic solution is possible only for very simple systems. Nevertheless, it may be possible to approximate the required behaviour by making judicious assumptions, but for that we need a deeper understanding of the relationship between biosynthetic enzyme E_1, its product A that connects it to the internal Michaelis-Menten reactions catalysed by E_2 and E_3, and allosteric modifier P. This chapter describes the results of the investigation into this relationship.

We have already shown that under conditions of flux control by demand the assumption of $\varepsilon_a^{v_1} \approx 0$ ensures that in the full supply-demand system the steady-state concentration $\bar{p}$ is completely determined by the properties of E_1. This means, of course, that E_1 has complete control of the biosynthetic flux (the flux local to the biosynthetic subsystem), as can be seen from setting $\varepsilon_a^{v_1}$ to zero in

$$C_1^{J_{\text{bio}}} = \frac{\varepsilon_a^{v_2}\varepsilon_b^{v_3}}{\varepsilon_a^{v_2}\varepsilon_b^{v_3} - \varepsilon_a^{v_1}\varepsilon_b^{v_3} + \varepsilon_a^{v_1}\varepsilon_b^{v_2}} \xrightarrow{\varepsilon_a^{v_1}\to 0} 1 \tag{4.1}$$

On the other hand, in the biosynthetic subsystem control over $\bar{a}$ and $\bar{b}$ under these conditions depends only on the properties of E_2 and E_3, as can be seen, for example, from setting $\varepsilon_a^{v_1}$ to zero in C_1^a and C_1^b

$$C_1^a = \frac{\varepsilon_b^{v_3} - \varepsilon_b^{v_2}}{\varepsilon_a^{v_2}\varepsilon_b^{v_3} - \varepsilon_a^{v_1}\varepsilon_b^{v_3} + \varepsilon_a^{v_1}\varepsilon_b^{v_2}} \xrightarrow{\varepsilon_a^{v_1}\to 0} \frac{\varepsilon_b^{v_3} - \varepsilon_b^{v_2}}{\varepsilon_a^{v_2}\varepsilon_b^{v_3}} \tag{4.2}$$

and

$$C_1^b = \frac{\varepsilon_a^{v_2}}{\varepsilon_a^{v_2}\varepsilon_b^{v_3} - \varepsilon_a^{v_1}\varepsilon_b^{v_3} + \varepsilon_a^{v_1}\varepsilon_b^{v_2}} \xrightarrow{\varepsilon_a^{v_1}\to 0} \frac{1}{\varepsilon_b^{v_3}} \tag{4.3}$$

Therefore, at any specific value of $\bar{p}$ the steady-state concentrations $\bar{a}$ and $\bar{b}$ are set by the properties of E_2 and E_3: the higher their activities, the lower $\bar{a}$ and $\bar{b}$. Theoretically, thermodynamic considerations set the minimum concentrations of $\bar{a}$ and $\bar{b}$ at any $\bar{p}$. If the equilibrium constants are K_2 and K_3, it follows that the minimum concentrations are

$$a = \frac{p}{K_2K_3} \qquad \text{and} \qquad b = \frac{p}{K_3} \tag{4.4}$$

Therefore, under near-equilibrium conditions the relationship between $\bar{a}$ or $\bar{b}$ on the one hand and $\bar{p}$ on the other should become nearly linear.

The assumption of near-equilibrium in reactions 2 and 3 would simplify the behaviour of the biosynthetic subsystem considerably. We could represent J_{bio} with the rate equation for E_1 and replace any occurrence of the concentration of its immediate product A with the expression $a = p/K_2K_3$. For example, if, as before, $K_2 = K_3 = 10$ (and $K_1 = 400$), the reversible Hill-equation used in Fig. 3.7 becomes

$$v_1 = \frac{\frac{200}{s_{0.5}}\left(s - \frac{p/100}{400}\right)\left(\frac{s}{s_{0.5}} + \frac{p/100}{a_{0.5}}\right)^{h-1}}{\left(\frac{s}{s_{0.5}} + \frac{p/100}{a_{0.5}}\right)^{h} + \frac{1 + \left(\frac{p}{p_{0.5}}\right)^{h}}{1 + \alpha\left(\frac{p}{p_{0.5}}\right)^{h}}} \tag{4.5}$$

4.1 The effect of varying the affinity of enzyme E_1 for its product A

Fig. 4.1 a shows that when binding of A to E_1 is very weak the reversible Hill equation (dotted grey curve) approximates the simulated steady-state flux (solid grey curve) quite accurately, while the simulated steady-state concentration $\bar{a}$ (solid black curve) is near equilibrium in the p-range from about 3 upwards (where the flux is low). So, of course, is $\bar{b}$ (not shown on the graph, but about ten times higher than $\bar{a}$). The reason why $\bar{a}$ increases considerably at low values of p is that the degree of saturation of E_2 by A must increase considerably to sustain the increased flux. The higher the $V_{\max}$ of E_2, the less the increase in $\bar{a}$ needed to carry the flux. We therefore predict that an increase in the activities of E_2 and E_3 should pull $\bar{a}$ down at low p (this prediction will be explored further on in Fig. 4.4).

We first ask ourselves what would happen if the binding of A by E_1 became stronger. Fig. 4.1 b–d shows what happens when $a_{0.5}$ decreases. At first, two aspects of what we found quite perplexed us. In Fig. 4.1 b there is a rate *activation* by p in both the simulation and the equilibrium-approximation (the same is found in the equilibrium-approximation in Fig. 4.1 c). This activation turns out to be quite easy to understand. In the numerator of the reversible Hill-equation, the reaction product occurs not only in the mass-action term $s - \frac{a}{K_{\text{eq}}}$ (where its increase will always decrease the rate), but also as a positive term in $\left(\frac{s}{s_{0.5}} + \frac{a}{a_{0.5}}\right)^{h-1}$. As shown by the grey dotted rate curves in both Fig. 4.1 b and c it is therefore possible that conditions exist where P can activate the enzyme. This phenomenon is not unique to the reversible Hill equation, but is to be expected in any rate equation where product concentration occurs in the numerator with a positive coefficient. For example, product activation is also displayed by reversible Monod-Wyman-Changeux rate equations [29] at low product concentrations.

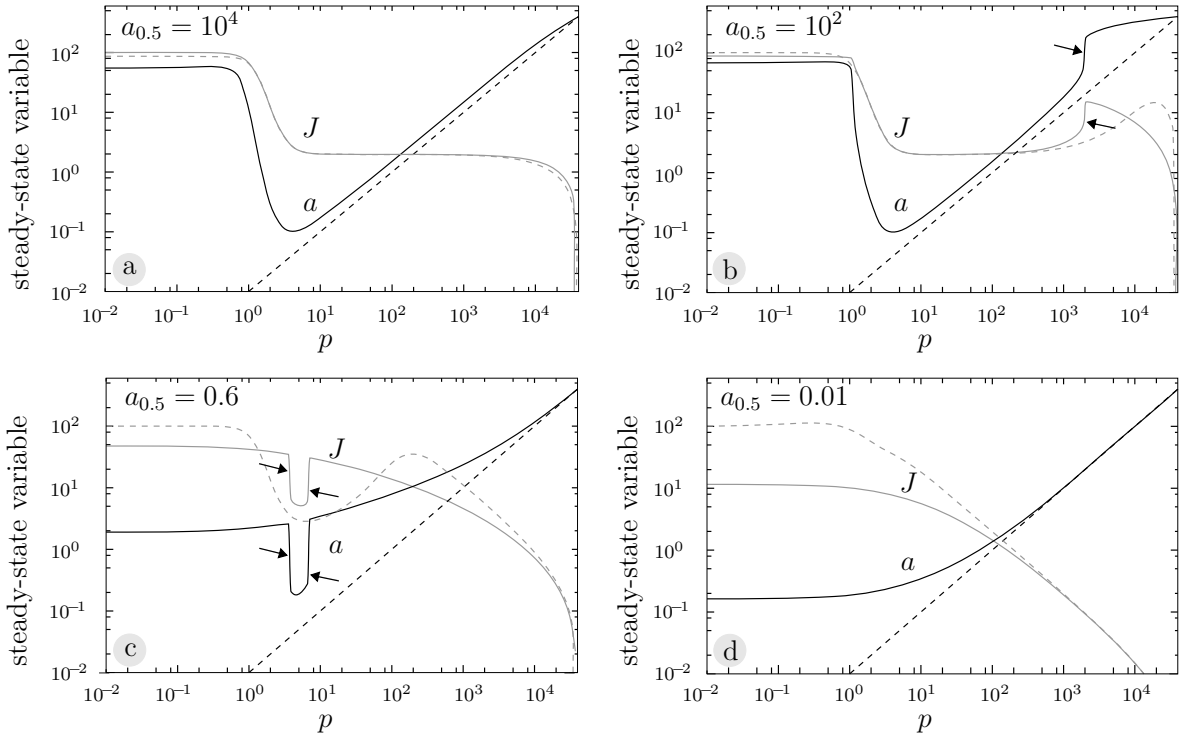

Fig. 4.1 *Approximating the behaviour of biosynthetic supply at different values of* $a_{0.5}$. Each of the graphs shows the concentration $\bar{a}$ in black and the flux in grey. The solid lines represent simulated steady-state behaviour, while the dashed lines represent the behaviour when a is assumed to be in equilibrium with p (as explained in the text). Arrows point to apparent discontinuities. Simulation conditions are as in Fig. 3.7, except that $V_2 = V_3 = 100$; the values of $a_{0.5}$ are shown on the graphs.

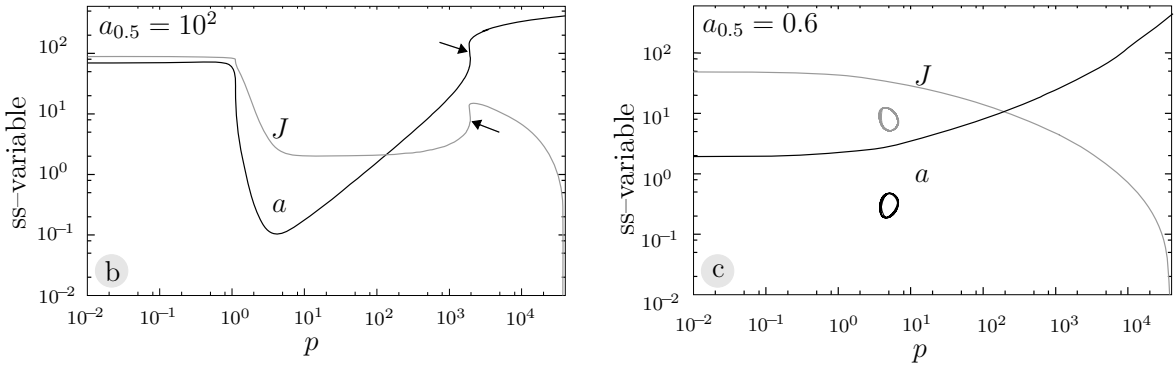

Fig. 4.2 *Remodelling Fig. 4.1 b and c with the Scamp continuation algorithm.* In b, notice how the jump is in actual fact a hysteresis which leads to the possibility of multiple steady states. c shows how the two jumps are really a ring that is called an isola.

The second perplexing aspect was that the simulated behaviour showed apparent discontinuities (indicated by the arrow in Fig. 4.1 b and c. At first we thought that this was an artifact or a bug in the simulation program Gepasi, but after checking and rechecking our models we were satisfied that this behaviour was real and reproducible. It clearly exists only in a limited range of $a_{0.5}$, because when $a_{0.5}$ is decreased even further to 0.01 (Fig. 4.1 d) then the curves become smooth again: the allosteric feedback effect of P is now overshadowed by the competitive product inhibition effect of A (compare with Fig. 3.8 b). The discontinuous behaviour is absent when near-equilibrium is assumed, although product activation is still present. This is probably the result of a always changing in a fixed proportion to p, and not being allowed to float freely.

It then occurred to us that the rate curves might be hysteretic with an unstable branch, so that Gepasi could not handle the transition gracefully. Fortunately, Scamp has a built-in continuation algorithm that can handle such situations[1].

4.2 Of mushrooms and isolas

Figs. 4.2 a and b show the results of re-modelling Fig. 4.1 b and c with Scamp's continuation algorithm. The arrows in Fig. 4.2 a point to a clear hysteretic profile with respect to p, albeit not very pronounced. The escarpment of the flux plateau ending at around $p = 1$ also seems to be non-monotonic. Fig. 4.2 b is decidedly more spectacular. It consists of two stable monotonic curves plus two circular curves known in the trade as 'isolas' (perhaps, in time to come, the 'Hofmeyr isola' after its discoverer).

At this stage we felt like Plato's cave-dwellers that catch only glimpses of reality by watching shadows on the rock face. However, to climb out the cave and view the full

[1]In *continuation* the scanned parameter (p in our case) becomes a dependent variable. A dummy parameter is introduced as the alternative independent variable and scanned. The effect of this transformation is that the S-shaped hysteretic curve in 2-dimensional space is now stretched into 3-dimensional space along a third axis representing the scanned dummy parameter. Any unstable branch in 2-D space now becomes a well-behaved stable branch in 3-D space.

reality turned out to be more complicated than expected. To get a clearer picture of the transition from low to high affinity of E_1 for A we wanted to construct a 3-dimensional plot by adding an axis for $a_{0.5}$. We could not produce the regularly gridded data needed for generating the 3-D plot with one simulation program: Gepasi can produce gridded data, but only for the stable parts of the curves; Scamp in continuation mode on the other hand can produce the full picture but, because p is now a variable, its values are not gridded. At any specific $a_{0.5}$ we could, however, generate a curve on a planar cross-section of the 3-D space from separately simulated sections of that curve. Roughly 20 megabytes and 48 data files later, we finally climbed out of our cave and saw the weird landscape in the bright light of day. And what a picture it was (Fig. 4.3).

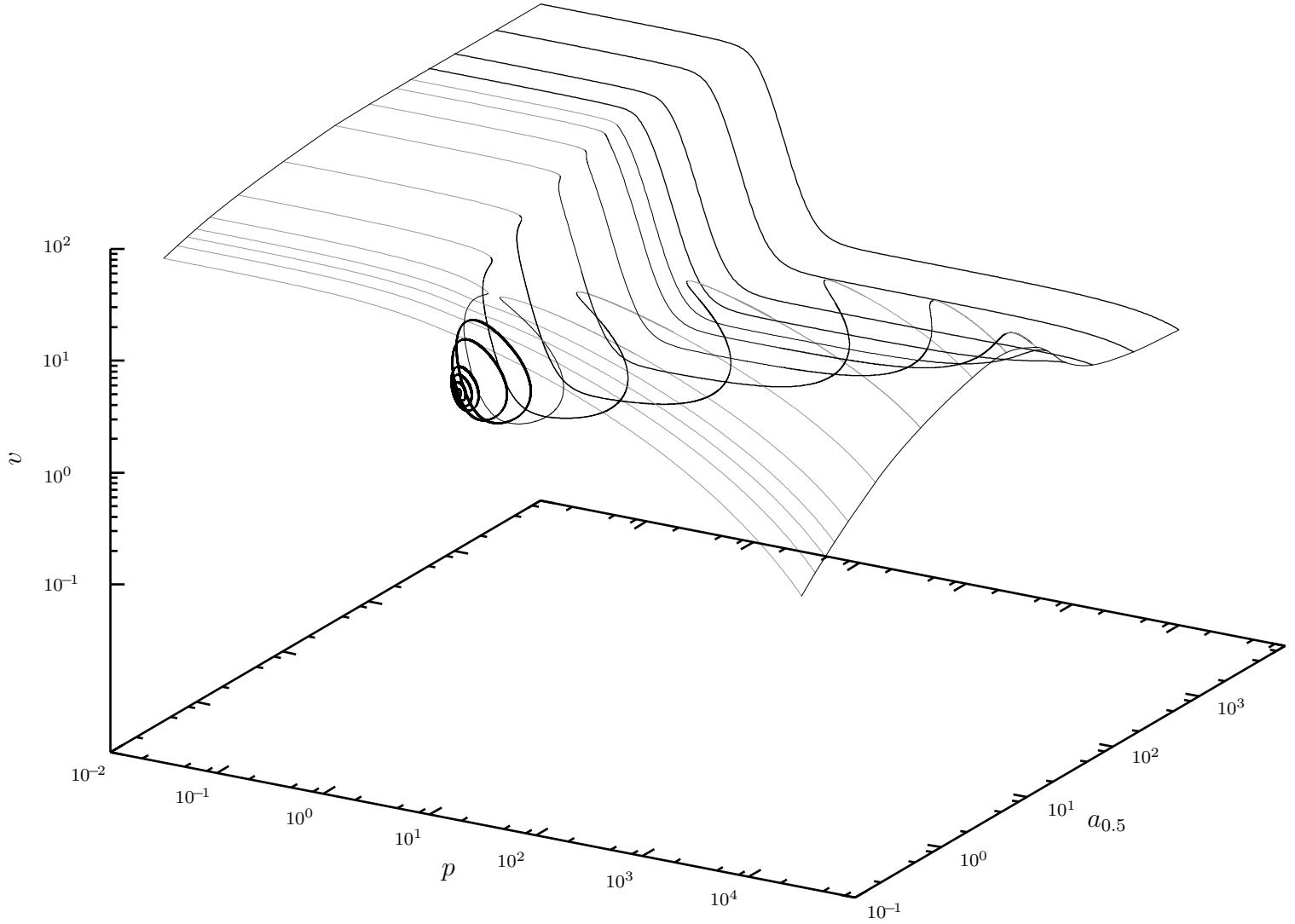

Fig. 4.3 *A 3-D picture of the mushroom transforming into a vanishing isola, with flux plotted against p at different values of $a_{0.5}$.* Similar graphs can be constructed for a or b: the shapes of the mushrooms and the isolas are different, but on the whole the same picture is found.

The figure shows how the smooth flux-inhibition curve at high $a_{0.5}$ gradually transforms into a double hysteretic curve (called a 'mushroom'—the 'Stellenbosch mushroom'?—albeit an upside-down one). The stalk eventually thins to nothing, pinching off the isola when the two bifurcation points meet, which in turn shrinks and eventually vanishes at $a_{0.5} = 0.5415$, leaving only the competitive product inhibition curve. We were excited that such a simple system could produce such a pretty and unexpected picture.

Beautiful and interesting as this behaviour may be, we do not want our designed system to exhibit it. How do we ensure the boring, but stable and desirable, response profile exemplified by Fig. 4.1 a? As we have already seen, one obvious solution is to decrease the sensitivity of E_1 to A. The other is to keep $\bar{a}$, and therefore, any inhibitory effect it may exert on E_i, as small as possible by pulling it down to near-equilibrium. The graphs in Fig. 4.4 show the effects on $\bar{a}$ of varying $a_{0.5}$ at different values of V_2 and V_3 (which we always keep at equal values), and *vice versa*.

Fig. 4.4 a corresponds to Fig. 4.1 a: very weak and very strong binding of A by E_1 eliminates the mushroomy behaviour that exists at intermediate values of $a_{0.5}$. Increasing the activities of E_2 and E_3 pulls down $\bar{a}$ to near-equilibrium values and also decreases and even virtually eliminates the increase in $\bar{a}$ at low p seen in graph a. Graphs d, e, and f show the effect of changing V_2 and V_3 at low, intermediate and high affinity of E_1 for A. Here it is particularly clear how an increase in V_2 and V_3 pulls $\bar{a}$ down to near-equilibrium.

Fig. 4.5 a shows that this minimising effect of high E_2 and E_3 activities on $\bar{s}$ ensures the appropriate steeply cooperative flux response at high $a_{0.5}$ and completely eliminates the activatory effect of P that is still evident at lower values of $a_{0.5}$. The graph in b shows that if binding of A by E_1 is strong, then not even high E_2 and E_3 activities can yield the desired response; although the inhibitory range does shift slightly the profile resembles that of gradual competitive inhibition.

4.3 Conclusions

These results indicate that in general, a near-equilibrium and approximately linear relationship between a or b and p cannot be assumed without losing important and interesting behaviour. However, it would be reasonable to say that under certain conditions, i.e., no communication (very weak binding) between e_1 and its product and a near-equilibrium state in the Michaelis-Menten enzyme block (E_2, E_3), a linear relationship between a and p may be assumed for a p-range down to $p_{0.5}$. Under specific circumstances it is therefore possible to model the behaviour of the biosynthetic supply with a single enzyme. In summary:

1. Weak binding (a large $a_{0.5}$) can result in a linear relationship between a and p provided that E_2 and E_3 are very active.

2. Changes in the V_f of E_2 and E_3 can be used to eliminate or accentuate discontinuous behaviour caused by upstream communication between A and E_1.

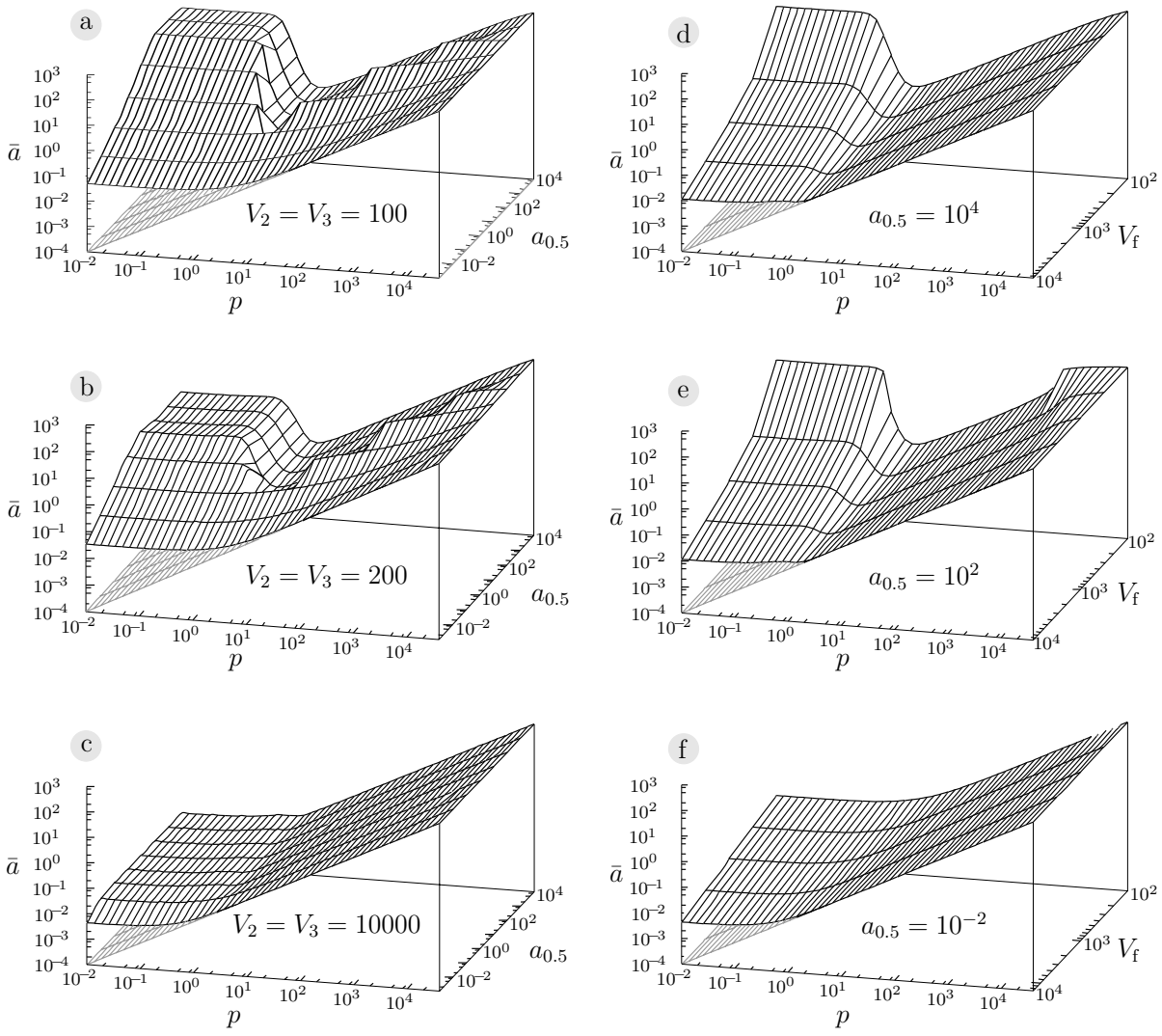

Fig. 4.4 *Combined effect of changing $a_{0.5}$ and the maximal forward rates of* E_2 *and* E_3 *on the steady-state concentration* $\bar{a}$. The left hand set of graphs have the V_{f}-values of E_2 and E_3 set, while $a_{0.5}$ is changed on the y-axis. The right hand graphs have $a_{0.5}$ set, while E_2 and E_3's V_{f} is changed along the y-axis. In each graph the grey surface corresponds the response when it is assumed that a and b are in equilibrium with p.

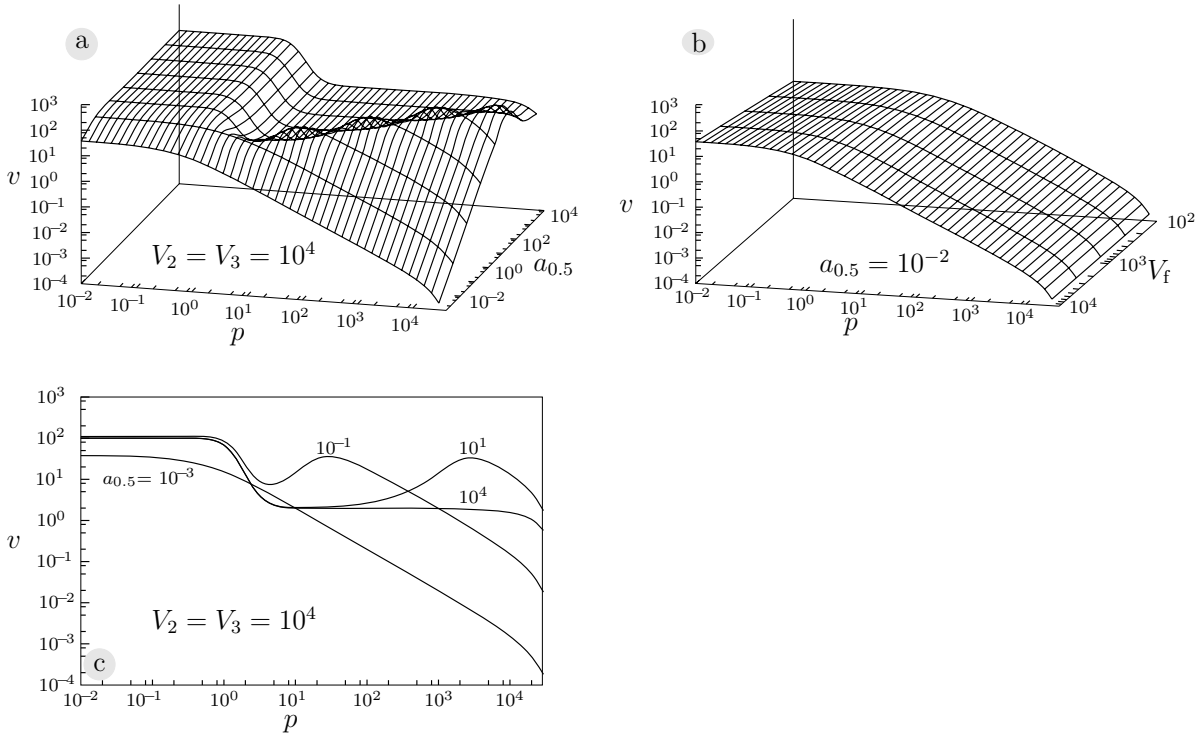

Fig. 4.5 *Combined effect of changing* $a_{0.5}$ *and the maximal forward rates of* E_2 *and* E_3 *on the steady-state flux* J_{supply}. The conditions in a and b correspond to those in Fig. 4.4 c and f. The graph in c is a two dimensional view of a at representative values of $a_{0.5}$ in which the activation effect of p on E_1 is particularly clear.

3. Very strong binding of A to E_1 also leads to a linear relationship over a wide range of E_2, E_3 activities but at the expense of homeostatic maintenance of $\bar{p}$ far from equilibrium.

We now return from our excursion to the main design process. In the next chapter we fine-tune the time-dependence of the supply response to changes in demand.

5 Tuning the transition time

In the design process thus far we have focussed mainly on the magnitudes and control of steady-state fluxes and concentrations of intermediates. Equally important though, is the time-scale within which metabolic processes operate. These temporal aspects are vital for any cell's survival, as they are indicative of the speed at which its metabolism can respond to changing conditions. In the context of the switching on and off of metabolic pathways, or their speeding up and slowing down, the time taken to make these transitions is of vital importance to the cell. Unfortunately, there are quite a number of proposed measures of transition time, all of which have advantages and disadvantages (cf. [30]). We shall only discuss one of them, the 'transition time' proposed by Easterby [31, 32, 33], which has been extended by Meléndez-Hevia and co-workers [34, 35, 36, 37].

5.1 'Transition time' as a state function

Consider a linear pathway in which a substrate S is converted through intermediates S_i and enzyme bound intermediates X_j to product P. Denote the sum of mass of all these *internal* species as $\sigma = \sum_i s_i + \sum_j x_j$. Mass conservation for the system means that the total matter input is accounted for as either free intermediate, bound intermediate, or product. If the input and the output is allowed to vary over time then it follows that at any time t the amount of matter inside the system is the difference between the amount that has entered and the amount that has left the system:

$$\int_0^t v_{\text{in}}(t) \cdot dt - \int_0^t v_{\text{out}}(t) \cdot dt = \sigma \tag{5.1}$$

The initial conditions at $t = 0$ are $v_{\text{in}} = v_{\text{in}}(0)$, $s_i = 0$, $x_j = 0$, $p = 0$, and therefore $v_{\text{out}} = 0$. We can split the integrals into: (i) a term $v(t) \cdot t$ that represents the amount of pathway substrate converted or product formed at time t had the initial rate been $v(t)$ that prevails at time t instead of 0, and (ii) a term that corrects this value for the fact that the relevant rate had actually changed from its initial rate to v(t) during that interval

$$\left(v_{\text{in}}(t) \cdot t - \int_{v_{\text{in}}(0)}^{v_{\text{in}}(t)} t \cdot dv_{\text{in}} \right) - \left(v_{\text{out}}(t) \cdot t - \int_0^{v_{\text{out}}(t)} t \cdot dv_{\text{out}} \right) = \sigma \tag{5.2}$$

which can be re-arranged to:

$$[v_{\text{in}}(t) - v_{\text{out}}(t)]\, t + \int_{v_{\text{in}}(t)}^{v_{\text{in}}(0)} t \cdot dv_{\text{in}} + \int_{0}^{v_{\text{out}}(t)} t \cdot dv_{\text{out}} = \sigma \tag{5.3}$$

(Note that we switched the limits on the integral with variable v_{in} to change its sign.) Fig. 5.1 gives a graphical interpretation of the derivation thus far.

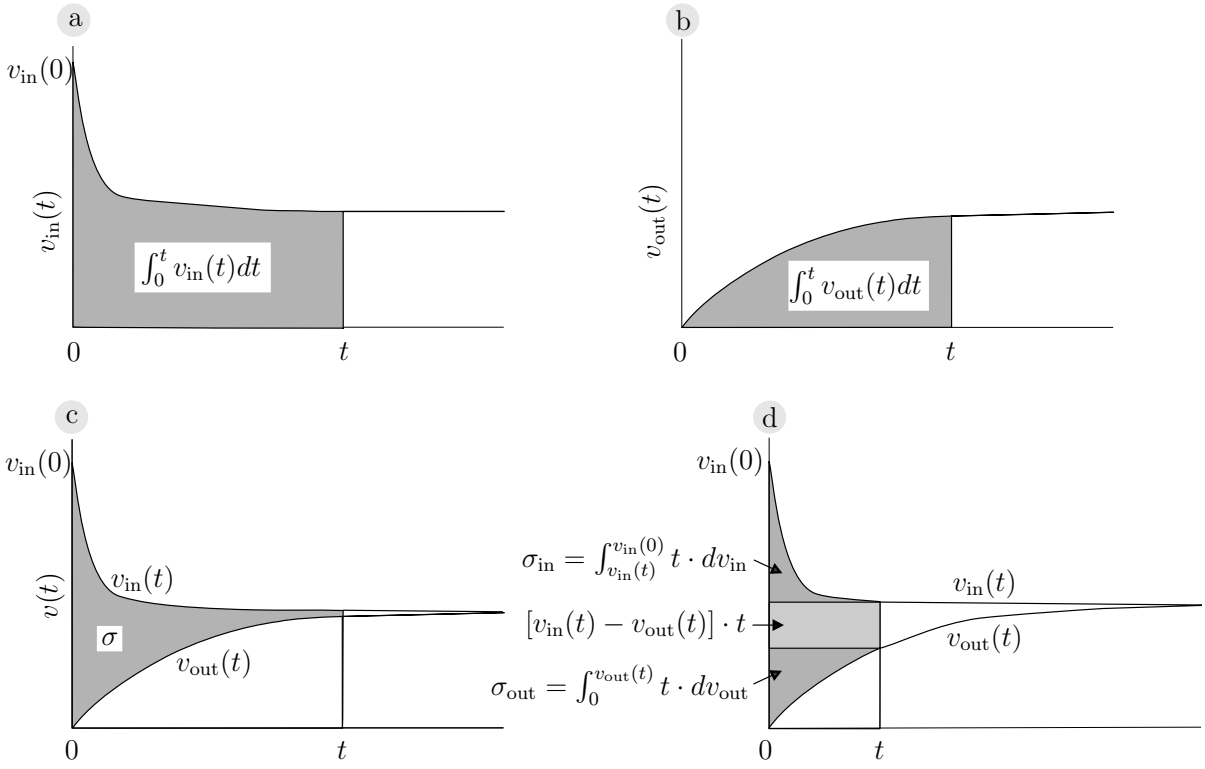

Fig. 5.1 *A graphical representation of the algebraic relationships in eqns. 5.1 to 5.3.* The areas under the curves in graphs a and b represent the integrals in eqn. 5.1, i.e., the mass that has entered the system via the input and the mass σ that has left the system via the output. The difference between these areas, i.e., the gray area in graph c, represents the mass that is pooled in the system itself. Graph d represents the terms on the left-hand side of eqn. 5.3 at time t.

Steady state is approached as $t \to \bar{t}$ where $v_{\text{in}}(\bar{t}) \approx v_{\text{out}}(\bar{t}) = J$ so that eqn. 5.3 simplifies to

$$\int_0^J \bar{t} \cdot dv_{\text{out}} - \int_{v_{\text{in}}(0)}^{J} \bar{t} \cdot dv_{\text{in}} = \bar{\sigma} \tag{5.4}$$

The time $\bar{t}$ is, however, not very useful as a transition time, because, mathematically speaking, a steady state is approached asymptotically, so that $\bar{t}$ is actually an infinite time. Nevertheless, one could define an approximate $\bar{t}$ in terms of, say, the time taken

for all rates to fall within 1% of the eventual steady-state flux (this can be called the 99% transition time τ_{99} (cf. [31, 38]).

The only way to define a 'transition time' τ that depends only on steady-state functions is as the time taken to turn over the internal pool $\bar{\sigma}$ completely at the prevailing steady-state flux with value J:

$$\tau = \frac{\bar{\sigma}}{J} \tag{5.5}$$

Note that this is in fact an exact definition of a *turnover time* (and we shall therefore use this term rather than transition time), but only an approximation of the time needed to reach steady state.

From Fig. 5.1 d is clear that $\bar{\sigma}$ can be split up into two components $\bar{\sigma}_{in}$ and $\bar{\sigma}_{out}$, which in turn leads to a split of the turnover time τ into

$$\tau = \tau_{\text{in}} + \tau_{\text{out}} = \frac{\bar{\sigma}_{\text{in}}}{J} + \frac{\bar{\sigma}_{\text{out}}}{J} \tag{5.6}$$

This can be given a clear graphical interpretation (Fig. 5.2). From this graph it can also be seen that τ_{in} is the turnover time when output rate is constant throughout, and, similarly, that τ_{out} is the turnover time when input rate is constant throughout.

As σ is the sum of the masses of all intermediates (molar concentration if stoichiometries are unitary), it also follows that the turnover time is the sum of the individual turnover times τ_i of all intermediary species, where

$$\tau_i = \frac{s_i}{J} \qquad \text{or} \qquad \tau_j = \frac{x_j}{J} \tag{5.7}$$

In the simulations described in this thesis, enzyme-bound intermediates are negligible so that their contribution may be safely ignored. Thus, for our system, the turnover time can be calculated as:

$$\tau = \frac{a + b + p}{J} \tag{5.8}$$

For a transition from a steady state with flux J_a to a steady state with flux J_b, Easterby [31, 32] derived the equation

$$\tau_{ab} = \tau_b - \left(\frac{J_a}{J_b}\right)\tau_a \tag{5.9}$$

where turnover times on the right hand side are for the establishment of steady state from an empty system.

Turnover times have the advantage that they can be calculated only from steady-state information, but the disadvantage that they do not incorporate any information about the transition between states. In our exploration of the time-dependent behaviour of the biosynthetic supply our system we shall have ample opportunity to assess the usefulness of this measure.

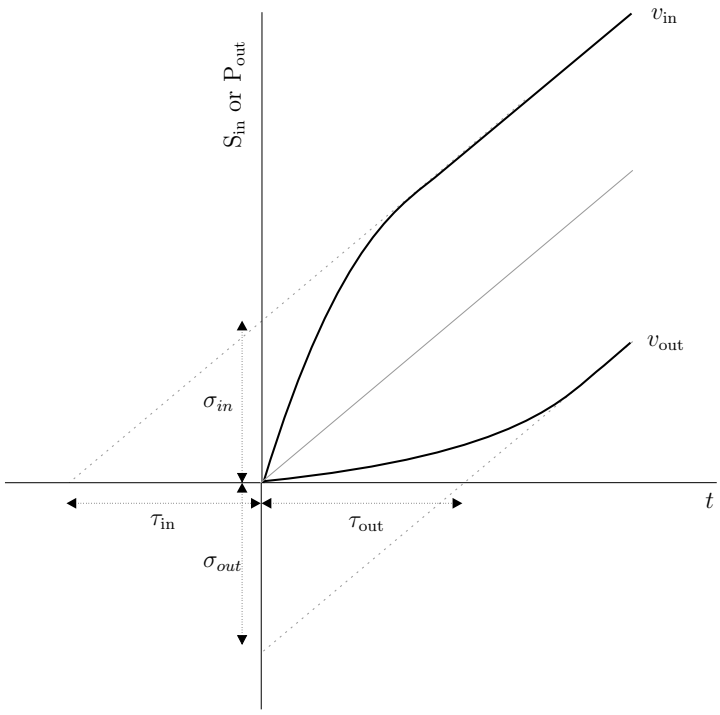

Fig. 5.2 *A graphical interpretation of the transition time for a system with varying input and output* [34]. The black curves represent the varying input (in terms of the amount of substrate, S_{in}, that has entered the system at any time) or output (in terms of the amount of product, P_{out}, that has left the system at any time), while the grey line represents either a constant input or constant output flux

.

5.2 The transient response of the biosynthetic supply to changes in demand

Let us now explore the transient response of the biosynthetic supply when it moves from one steady state to another: a 'high' steady state with a flux of 60, and a 'low' steady state with a flux of 1. As we have designed our system in such a way that the demand controls the flux, we set the flux simply by adjusting the activity of the demand. Let us review the relevant design criterion:

The system must respond *rapidly* to changes in the internal demand.

Fig. 5.3 shows how the system responds to an instantaneous transition from a high to a low (grey curves) and a low to a high (black curves) demand at time zero. Two properties of the supply system that could influence its transient response are investigated: (i) the presence (a and b) or absence (c and d) of allosteric end-product inhibition, and (ii) lower activities (a and c) versus higher activities (b and d) of E_2 and E_3.

The first marked effect of the presence of end-product inhibition is the rapidity of the transition, the new steady state being reached within 0.1–10 time units depending on whether the transition is from high to low or from low to high flux. Without end-product inhibition the transition takes 10^3 to 10^4 time units. The second marked difference is the concentration range within which a, b, and p move: 0.02 to 4 concentration units in the presence of end-product inhibition, compared with 10^2 to $\approx 4 \times 10^4$ (the near-equilibrium value of p) in its absence. The rapid response results both from the direct communication of P with the first enzyme in the sequence and from the small pool sizes and pool size changes that ensure a short transition. In the absence of end-product inhibition the pool size changes are orders of magnitude higher and take much longer, especially in Fig. 5.3c following a decrease in demand (the grey curves). In addition, changes in demand must be communicated up the chain via P, B, and A to E_1, instead of directly via P to E_1.

The effects of an increase in the activities of E_2 and E_3 on the transition time is much less clear. In some situations, e.g., the transition from high to low flux in the absence of end-product inhibition (the grey curves in c), the transition time decreases when V_2 and V_3 increases (the grey curves in d). However, this profile is apparently reversed when end-product inhibition is present (compare the grey curves in a with those in b). The transition from low to high flux confuses the issue even further (compare the black curves in a with those in b, and the black curves in c with those in d). Nevertheless, some of these results can be explained quite easily: for example, upon a decrease in demand in the absence of end-product inhibition the transition time must depend largely on how fast the feeding reactions fill up the intermediary pools to their new steady-state value; the results bear this out: with lower activity (the grey curves in c) it takes much longer to reach the new steady state than with high activity (the grey curves in d).

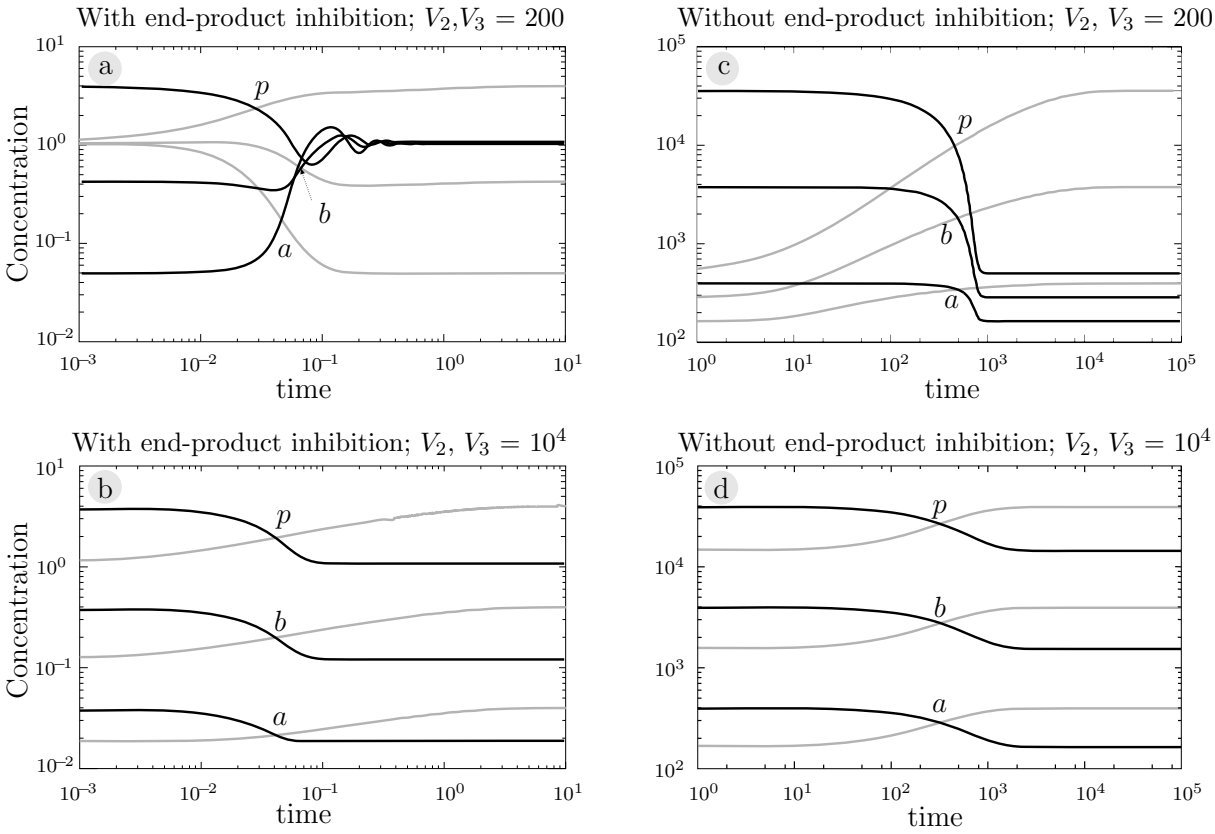

Fig. 5.3 *The transition between steady states at low demand (V_{dem} = 1) and high demand (V_{dem} = 60) and vice versa. A comparison between systems with and without end-product inhibition.* In graphs a and b there is end-product inhibition of E_1 by P ($\alpha = 0.001$), while in graphs c and d there is none ($\alpha = 1$). In a and c enzymes 1, 2 and 3 have $V_f = 200$ (the values used in all other simulations), whereas in b and d the V_f of enzymes 2 and 3 has been increased to 10^4. Other parameter values are as before. All four graphs show the transient changes in intermediate concentrations following an instantaneous transition from a low to a high (black lines) and a high to a low demand activity (grey lines) at time zero.

In contrast, the activities of E_2 and E_3 clearly affect the intermediate steady-state concentrations in a consistent manner: the higher their activities, the closer to equilibrium the p/b and b/a ratios. In Fig. 5.3 a and b, where P inhibits E_1, the steady-state concentrations of P do not depend on the activities of E_2 and E_3, but are set by the properties of E_1 (because $\varepsilon_a^{v_1}$ approximates zero by design). However, the steady-state concentrations of A and B are markedly affected: high activities of E_2 and E_3 pull down $\bar{a}$ and $\bar{b}$ to their near-equilibrium values where $\bar{p}/\bar{b} \approx 10$ and $\bar{b}/\bar{a} \approx 10$, and also dampens any oscillatory behaviour evident at the lower activity of E_2 and E_3. In the absence of end-product inhibition, the steady-state concentrations of A, B, and P are all close to equilibrium with S at low flux. At high flux all three concentration decrease, the magnitude depending on the values of V_2 and V_3; the higher these activities the smaller the change in the pools.

Increases in V_2 and V_3 can also have a smoothing effect on the transition profile, especially in the presence of end-product inhibition where, as is clear from Fig. 5.3 a, the progress curve can oscillate. We explored this behaviour more carefully by simulating the system subject to end-product inhibition with a larger number of intermediary values of V_2 and V_3, starting at 100, which is equal to the maximal rate that E_1 can attain at an $s/s_{0.5}$-value of 1 (Fig. 5.4). As V_2 and V_3 increases the metabolite profile for the transition from high to low flux is progressively smoothed, with increased damping of oscillations. Again the steady-state concentration of P is clearly not influenced by changes in the activities of E_2 and E_3, even though $\bar{a}$ and $\bar{b}$ vary considerably, especially at high flux. The reason is that the affinity of E_1 for A is so low ($a_{0.5} = 10^4$) that even at the highest concentration reached by A (≈ 10), E_1 can only be 0.001% saturated by A (in the absence of S). Therefore, $\varepsilon_a^{v_1} \approx 0$ under all simulation conditions. These graphs, much more than the graphs in Fig. 5.3 a and b, also show that the for A, B, and P transition time decreases with increasing V_2 and V_3 . This trend is not as clear for the transition from low to high flux, but, from a metabolic designer's point of view, high V_2 and V_3 always lead to smoother transitions and lower steady-state concentrations of intermediates, especially at high flux.

In the discussion thus far, we have been used visual estimations and comparisons of the time it takes to move between steady states. Are turnover times, discussed in the introductory section to this chapter, useful measures of these transition times? Using Gepasi and eqn. 5.9 we calculated the turnover times from high to low and low to high flux (Table. 5.1).

	End-product inhibition ($\alpha = 0.001$)		No end-product inhibition ($\alpha = 1$)	
	High to low	Low to high	High to low	Low to high
$V_{2,3} = 200$	3.4	0.06	38773	646
$V_{2,3} = 10^4$	3.2	0.05	27788	463

Table 5.1 *Absolute values of the turnover times calculated for the transitions in Fig. 5.3.*

Being state functions, the tabulated turnover times of course contain considerably less information than the simulations. What is clear though, is that both the simulated

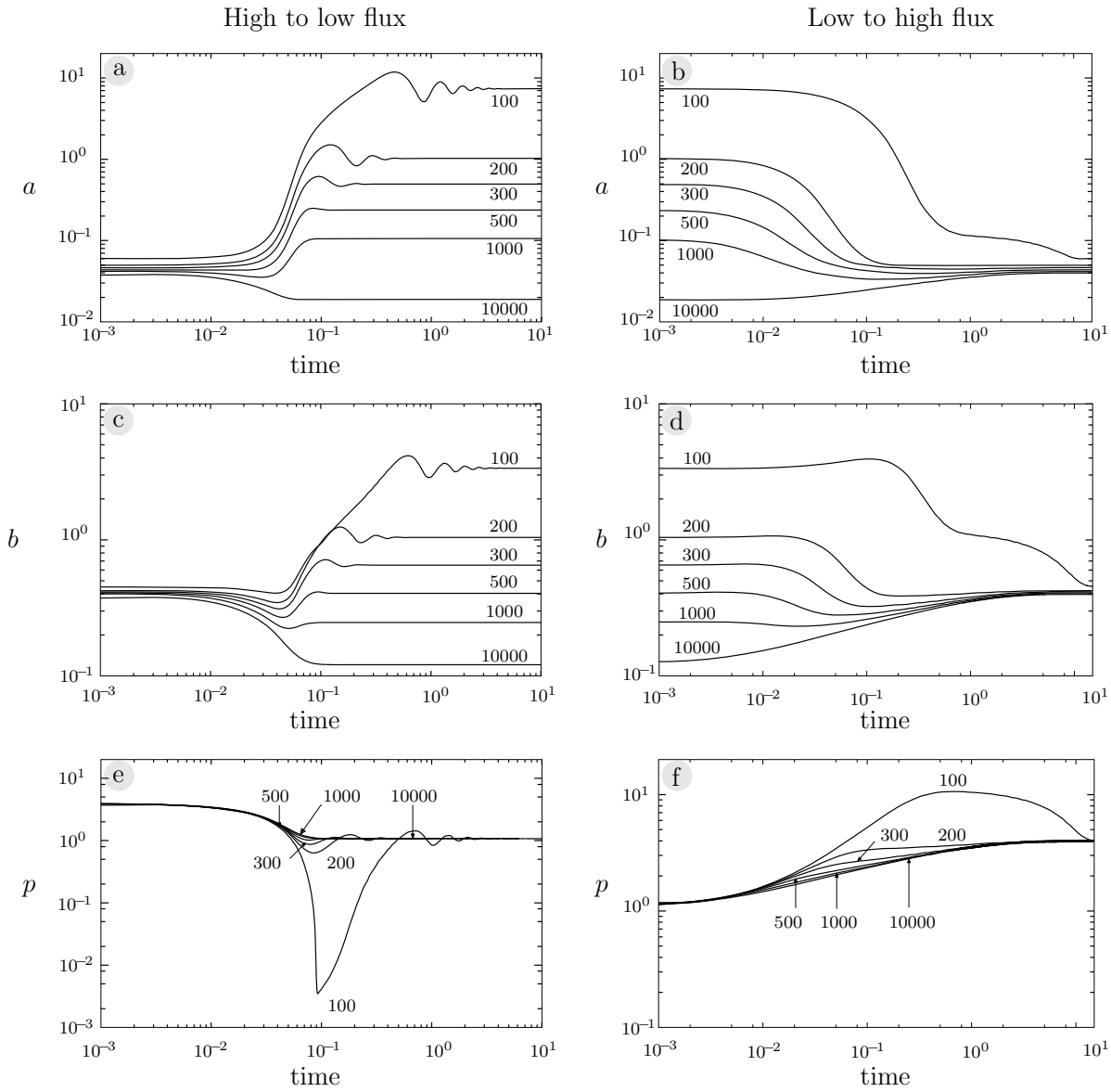

Fig. 5.4 *The transition between steady states at low demand ($V_{dem} = 1$) and high demand ($V_{dem} = 60$) and vice versa in a system with end-product inhibition ($\alpha = 0.001$).* The V_{f} of enzymes 2 and 3 have been set to the same value (indicated on the graph).

transitions and the calculated turnover times are much more rapid in the presence of end-production inhibition than in its absence; it may therefore be tempting to say that a long turnover time indicates a slower transition, while a short turnover time indicates a faster transition. Although, at first glance it may also seem that, in relative terms, the calculated turnover times are similarly good relative indicators of the time it takes to move between steady states, irrespective of whether end-product inhibition is present or not, this turns out not to be true. The calculated turnover times for transitions from high to low flux are about 60 times longer than for the transitions from low to high flux; this may roughly agree with the picture obtained in Fig. 5.3 b and c, but is difficult to reconcile with a, and clearly not true for d.

From the results shown in this chapter it appears that the best performance during steady-state transitions is obtained when P inhibits E_1, while E_2 and E_3 are active enough to keep a and b at low near-equilibrium concentrations. This ensures that any oscillations are damped and that the transitions take place as fast and as smoothly as possible. For our overall design process, this is a very promising result, because it fits in with what we have already established in the previous chapter, i.e., if we increase the activity of E_2 and E_3, thereby creating near-equilibrium conditions in the biosynthetic supply, we obtain a linear relationship between A and P and may model the whole block as a single reaction with reversible and allosterically modifiable Hill kinetics.

6 Completing the 4-way junction

We have now designed the core of the 4-way junction in such a way that, even without the rest, it functions independently and effectively. In this chapter we add catabolic demand and external supply. The idea is to explore only the broad outlines of the behaviour of the full system, without considering the details of the internal properties of these extra branches. In this chapter we model each branch of the 4-way junction with a single rate equation (we have justified our use of the reversible Hill equation as a model biosynthetic block in Chapter 4). Fig. 6.1 gives the kinetic details of this model.

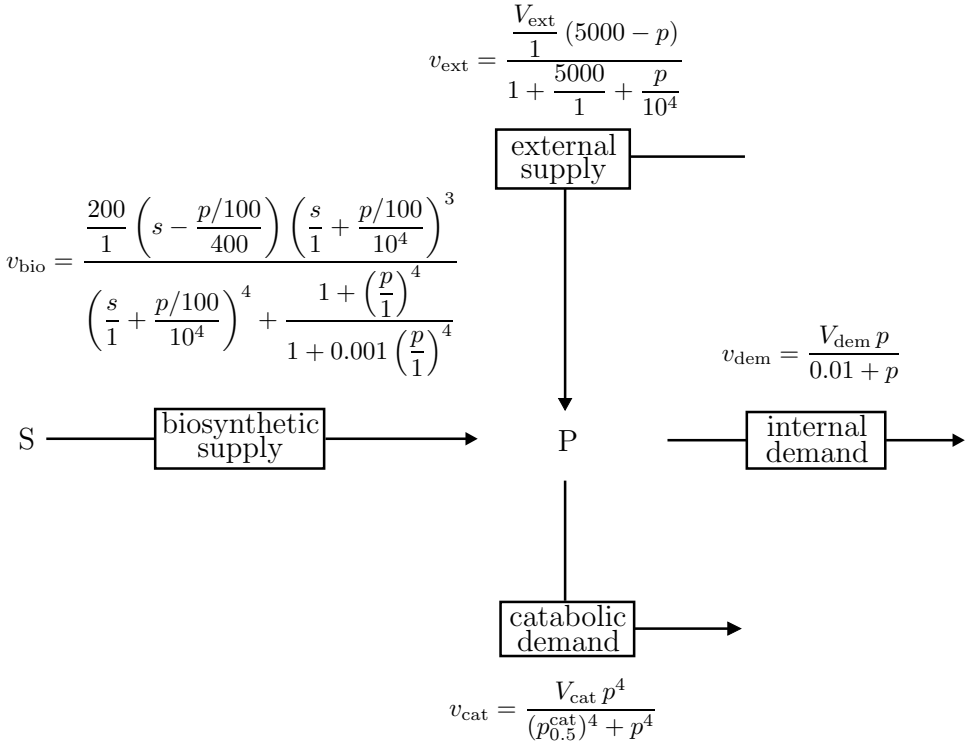

Fig. 6.1 *Modelling the 4-way junction with single rate equations for each branch.* The parameter values that will not be varied in our analysis are given directly in the rate equations. Catabolic demand is modelled with an irreversible Hill-equation, while the external supply rate equation is an instance of $v_{ext} = (V_{\text{ext}}/K_{\text{ext}})\,(p_{\text{ext}} - p_{\text{int}})\,/(1 + p_{\text{ext}}/K_{\text{ext}} + p_{\text{int}}/K_{\text{int}})$, i.e., assuming facilitated diffision for the uptake process and a high external substrate concentrations.

6.1 Catabolic demand as an overflow valve

Let us review the criterion that relates to catabolic demand:

> The catabolic demand should not operate at P concentrations in the normal working range, but should act as an overflow valve when P increases for some reason, such as external oversupply of P or extremely low demand for P. This would allow externally supplied P to be used as a source of energy.

We first concentrate on the overflow valve function. There are two main reasons why the P-pool can increase to high levels. The first is when P is oversupplied from outside; the second is when demand is so low that the lower regulatory limit of the biosynthetic block is breached and the system jumps from the region of kinetic regulation to that of thermodynamic regulation (this is clearly shown in Fig. 3.10 b on p. 42 in the jump from steady state 3 to 4). We first concentrate on making the catabolic demand prevent this last situation.

Fig. 6.2 shows the behaviour of the 3-way junction in which a catabolic demand has been added to the basic biosynthetic supply–internal demand system. These graphs should be read in conjunction with Fig. 6.3, which is a schematic and quantitative representation of the steady-state fluxes and concentration of P. In fact, the right-hand column shows the situation that we want to prevent (in the absence of catabolic demand). In graphs a, c, and e the demand is low and the steady state in the absence of catabolic demand is at a near-equilibrium concentration of P. When $p^{\text{cat}}_{0.5}$ is small (= 1) the steady-state concentration of P is reduced dramatically, but at the cost of creating a high catabolic demand which the supply must now also satisfy (an energetically unfavourable situation; see the diagram marked a in Fig. 6.3). Even when the demand increases (graph b) their is still substantial wastage down the catabolic demand. A much more favourable situation is created when the $p^{\text{cat}}_{0.5}$ is increased so much that the catabolic rate curve intersects with the biosynthetic rate curve just beyond the lower limit of kinetic regulation ($p^{\text{cat}}_{0.5} = 50$ in graph c). Here the catabolic demand prevents the jump to the near-equilibrium arm, creating a minimal extra demand that biosynthesis must satisfy. The only effect of any further increase in $p^{\text{cat}}_{0.5}$ (say to 1000 in graph e) is to increase the steady-state concentration of P and is therefore undesirable. At these higher values of $p^{\text{cat}}_{0.5}$ an increase in the internal demand (graphs d and f) effectively switches catabolic demand off by pulling $\bar{p}$ down to levels far beyond the $p^{\text{cat}}_{0.5}$.

Fig. 6.3 includes a few extra views on the behaviour of the above system at very high demand. The second row shows the limit of the range where supply can still just meet demand (the extra presence of catabolism makes little difference to this specific system). In the top row the demand is much higher than what the supply can meet, and supply now limits and controls the steady state flux. The steady-state concentration of P is so low that the catabolic demand does not function at any of the values of $p^{\text{cat}}_{0.5}$ that we consider.

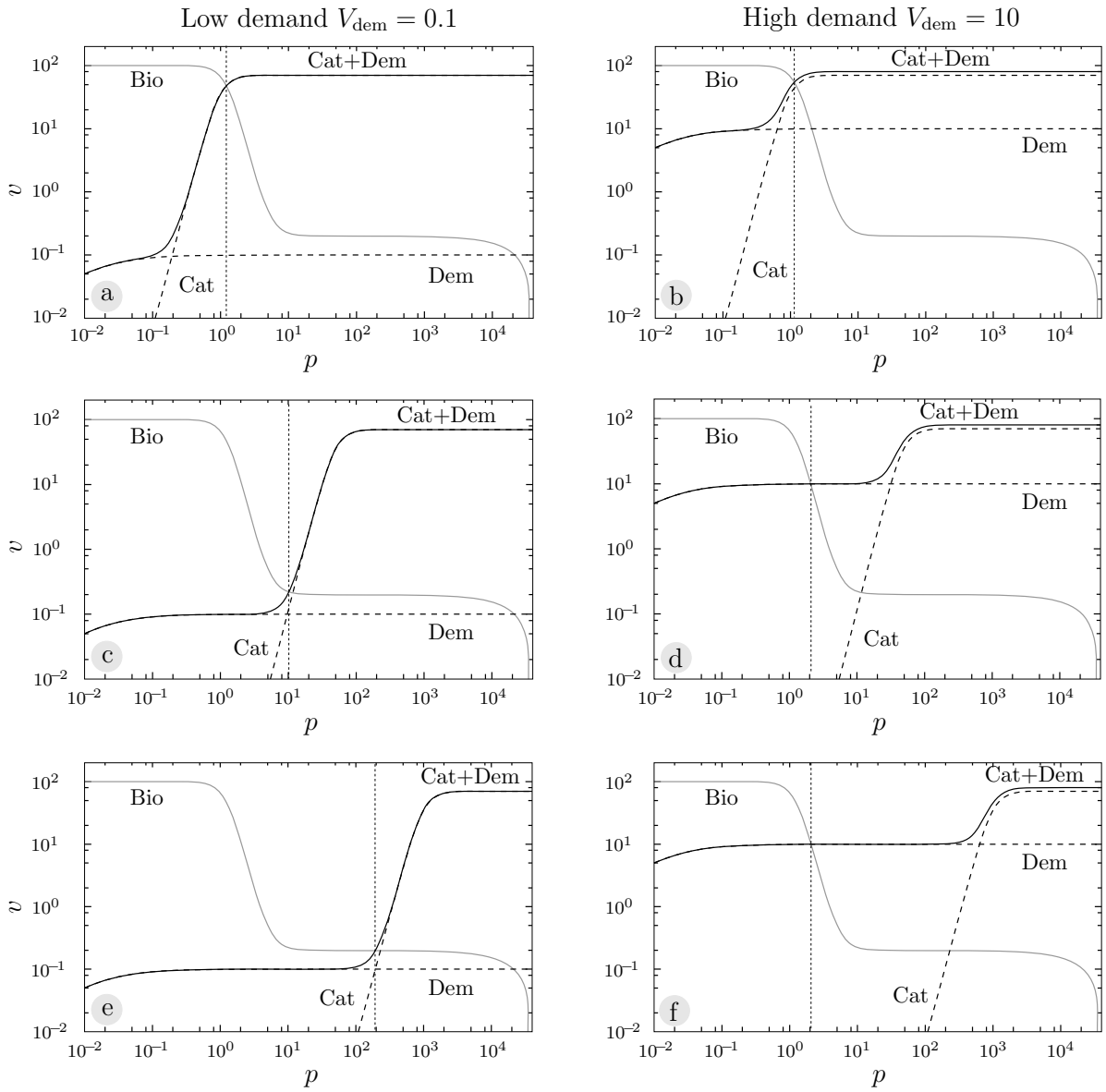

Fig. 6.2 *The effect of varying $p_{0.5}^{\mathrm{cat}}$ on the efficacy of catabolic demand as an overflow valve at low demand activity.* The limiting catabolic rate V_{cat} is set 70, while the half-effect parameter $p_{0.5}^{\mathrm{cat}}$ has the following values: a, b: 1, c, d: 50, e, f: 1000. The two demands are represented by dotted curves, while their sum is the solid black curve. The grey curve is the rate of biosynthetic supply. The solid curves intersect at the steady state, which is shown by a vertical dotted line. Steady-state fluxes obtain where this line intersects with the different rate curves.

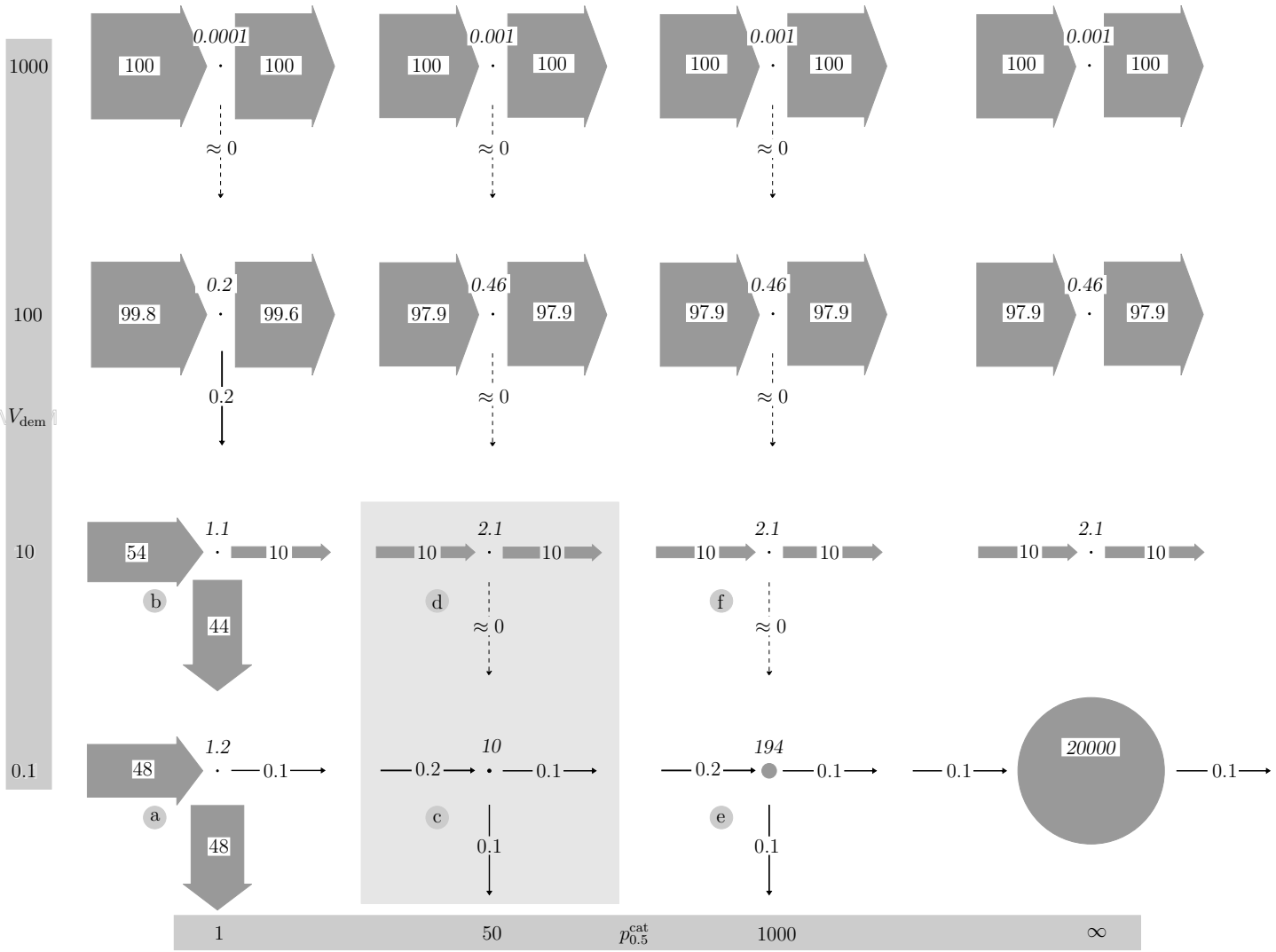

Fig. 6.3 *A schematic representation of the steady-state fluxes and concentration of P at various combination of* $p^{\mathrm{cat}}_{0.5}$ *and* V_{dem}. The arrows conform to the scheme in Fig. 6.1. The width of the arrows and the circle areas reflect the relative sizes of the steady-state fluxes and concentration of P. The schemes marked (a)–(f) correspond to the graphs in Fig. 6.2. Also shown are the steady states at much higher demands, the top row exceeding the supply rate capacity by a factor of 10, and the second row equalling the supply rate capacity. The right-hand column represents the supply-demand system in the absence of catabolic demand and is included for comparison. The shaded region shows the optimal choice of $p^{\mathrm{cat}}_{0.5}$.

In the above, the limiting catabolic rate has rather arbitrarily been set to 70 and the Hill-coefficient to 4. Although these two parameters do of course affect systemic behaviour, they are much less important than $p_{0.5}^{\text{cat}}$, which, as we have seen, must be specifically adjusted to have the desired effect. Nevertheless, the activity of the catabolic demand should at least be such that the combined catabolic and internal demand rate intersects with the biosynthetic rate in the region where the supply is kinetically regulated or just beyond it. Clearly the steeper the catabolic rate response to p (the higher the Hill-coefficient), the better, but this is not so crucial. We leave our investigation of the properties of the catabolic demand at this, being satisfied that we know how to improve the system even further with respect to the stated design criterion.

6.2 If ready-made product is available

We now freeze the $p_{0.5}^{\text{cat}}$ of the catabolic demand at the optimal value of 50, and consider what the system does when P is supplied from an external source (Fig. 6.4). The design criterion that must be met is:

Biosynthetic supply should be switched off if P can be supplied from the external environment. The intuitive argument that lies at the basis of this criterion is that this should save on energy and reducing power usually needed for bio synthesis.

In addition we must also keep in mind that the catabolic demand must act as an overflow valve when there is an external oversupply of P (the previous section dealt only with catabolic demand as overflow valve for increased $\bar{p}$ as a result of very low demand).

Fig. 6.2 d has been repeated as Fig. 6.4 a for the sake of convenience. In graph b an external supply with high external concentration of P has been added. The solid grey line shows the new combined supply. Steady state now obtains at about 10^3-fold higher $\bar{p}$. The internal demand is still satisfied and the biosynthetic supply is practically switched off. As shown clearly by the scheme on the right-hand side of b, most of the external supply now flows into the catabolic demand. The size of the P-pool has, however, increased by a factor of 500. To ensure a steady state at lower $\bar{p}$ we can increase the activity of the catabolic demand (as in graph c). This has little effect on the flux profile, but causes a 20-fold decrease in $\bar{p}$. The catabolic demand in c now satisfies both its design criteria: In the absence of external supply it prevents increases in $\bar{p}$ caused by a demand that is lower than the regulatory limit of the biosynthetic supply; in the presence of external supply it acts as an overflow valve and keeps the inevitable increase of $\bar{p}$ to a minimum. In d the catabolic demand is left out: the system is at the mercy of external supply, and although internal demand is met and biosynthetic supply is switched off, the huge dam of P that forms can only have disastrous consequences.

We shall not explore further the effect of changes in V_{ext} or of different external supply kinetics, being satisfied that we have learnt that V_{cat} must be adjusted to compensate for this, whereas the value of $p_{0.5}^{\text{cat}}$ should be set according to the lower regulatory limit of the biosynthetic supply.

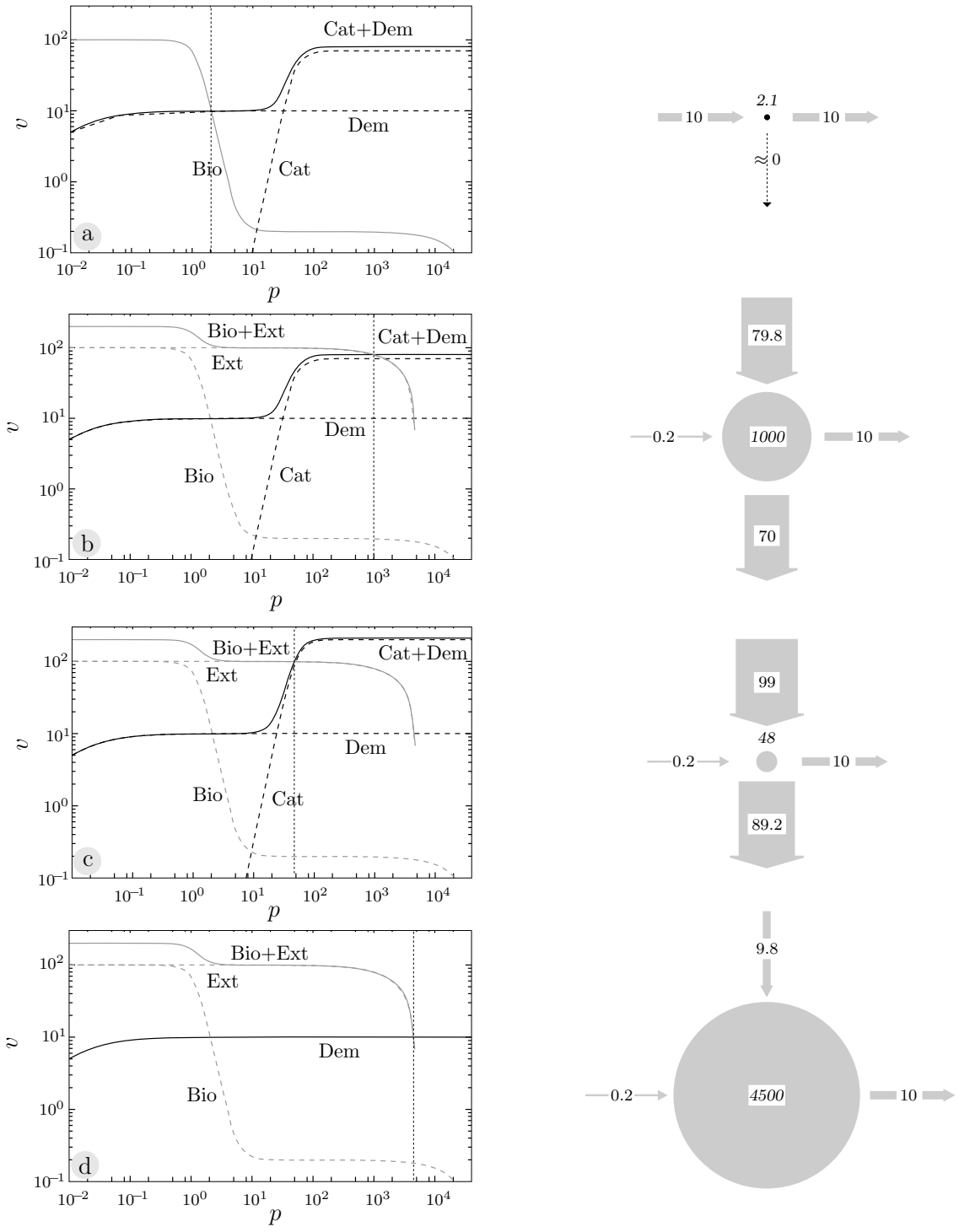

Fig. 6.4 *Adding an external supply to the 3-way junction.* a The 3-way system containing an optimal catabolic demand ($p^{\text{cat}}_{0.5} = 50$ and $V_{\text{f}} = 70$); the same as Fig. 6.2 d. b The system in a to which an external supply (V_{ext}= 100) has been added. c V_{cat} has been increased to 200. d The system with external supply and no catabolic demand. The arrows in the right-hand-side schemes conform to the scheme in Fig. 6.1. The grey curves show the supply reactions and the black curves the demand reactions (dotted: individual blocks; solid: combined blocks). The vertical dotted line indicates the steady state.

Here we end our journey. The road goes on, however, and there are numerous byways that we have passed and left unexplored. We hope our work shall inspire others to follow this approach to understanding the design and behaviour of metabolic networks and other cellular processes. In the last chapter we take a bird's-eye view of what we have achieved and discovered.

7 Discussion

As discussed in Chapter 1 we tackled this project in the hope of transforming ourselves into better 'reverse-engineers of life' and of gaining a deeper understanding of which properties of metabolic systems determine which functions. In fact, we can also view what we have been doing as studying functional differentiation in metabolic reaction networks.

To our knowledge the study of function and functional differentiation in reaction networks has seldom been approached explicitly from the point of view of 'forward engineering'. In fact, the only other study that we are aware of is that of Acerenza [39, 40, 41]. He has developed a strategy called 'metabolic control design' that attempts to find answers to matters such as the construction of a metabolic system that shows a pre-established pattern of responses, or the way that constraints operating during evolution shape metabolic responses. He uses the network of chemical transformations and the desired pattern of responses as input, and the output the kinetic properties of the component enzymes that are required for this purpose. In essence, he specifies a control profile, calculates the elasticity coefficients and then tries to work back to the kinetics. Although Acerenza's strategy may bear fruit in the future, it needs to be developed further and applied before its utility becomes obvious. In part our approach also moves back and forth between the control, elasticity, and kinetic levels, but it is enriched by consideration of how the steady state itself changes over large ranges of parameter variation, by functional interpretation in terms of a quantifiable definition of regulation, by viewing the network as a nested system. We believe that an analysis as set out in this thesis has led to a much deeper level of understanding than what would emerge from a control design study only.

We have succeeded in designing a metabolic system to perform a predefined set of functions in such a way that each function can be attributed to one step or to a group of steps in the system. It is interesting that a distinct 'pecking order' of functions emerged:

1. Flux-control by demand is ensured by a zero elasticity to its immediate substrate, P, the product of the biosynthetic block;

2. This has the inevitable consequence that concentration control of P becomes a function of the biosynthetic block. Furthermore, it is possible to localise this function in a biosynthetic enzyme with which P interacts directly: this could be the last enzyme for which P is a direct product or the first enzyme in the reaction sequence leading to P. When, for example, P feeds back onto the first enzyme, the

condition $\varepsilon_a^{v_1} \approx 0$ ensures that it completely determines both the level of P (at a set demand) and the steepness of the p-response to changes in demand;

3. If $\bar{p}$ is set by the properties of E_1, then the other biosynthetic enzymes (E_2 and E_3) determine the steady-state concentrations of the biosynthetic intermediates. The more active the enzymes, the lower these intermediate concentrations are as they tend to their near-equilibrium values;

4. The presence of end-product inhibition and the near-equilibrium condition of the intermediate steps ensures a rapid transition from one steady state to another following a change in demand.

We now not only understand exactly which properties of the enzymes determine which systemic functions, we have also discovered which properties lead to 'dangerous', albeit interesting behaviour. For example, eating the 'mushroom' of strong product (A) binding to E_1 caused visions of strange structures in state space (4).

We have demonstrated how integrated use of all our design tools (control analysis, enzyme kinetics, rate characteristics, simulation) leads to deep understanding of the behaviour of metabolic networks. We could not have achieved this level of understanding with any one of these tools alone. We hope that this exercise can serve as an example for similar future studies.

What has been described here is of course just the first part of a continuing process. The understanding gained here can serve as framework for studying real systems experimentally or for re-interpreting existing experimental data. It may turn out that the functional criteria that we designed are not necessarily the ones that Nature selected for. This, however, does not nullify what we have learnt. When you learn to design for what you regard as a desirable property A, you inevitably learn how to avoid what you regard as an undesirable property B. If it turns out that B is actually the property you want you already know to confer it. For example, if we want our biosynthetic system to exhibit hysteretic behaviour we know which parameters of E_1 we should tweak and to what degree.

In summary, we hope that the work presented in this thesis us some distance along the path of reconciliation asked for in the following:

> First, one cannot escape the conclusion that the organism (in its development and function) reacts as a unitary whole. Secondly, one cannot ignore the fact that in spite of this recognized unitary wholeness, a great number of processes in the organism can be explained as a fixed linear sequence of component processes, i.e. through mechanisms. These two facts have to be reconciled now.
> Paul Weiss, Yearbook Society of General Systems Research (1959).

We hope, with Herman Weyl, that the beauty and simplicity that we have unearthed in the behaviour of a rather simple system also turns out to be true:

> My work has always tried to unite the true with the beautiful and when I had to choose one or the other, I usually chose the beautiful.
> Hermann Weyl, quoted in an obituary by Freeman J. Dyson in Nature, March 10, 1956.

In this regard, Richard Feynman's observation is encouraging:

> It is possible to know when you are right way ahead of checking all the consequences. You can recognize truth by its beauty and simplicity. Richard Feynman, *The Character of Physical Law*, M.I.T. Press, Cambridge and London, 1965.

8 Bibliography

[1] Kacser, H., Burns, J. A., and Fell, D. A. (1995). *Biochem. Soc. Trans. 23*, 341–366.

[2] Heinrich, R. and Rapoport, T. A. (1974). *Eur. J. Biochem. 42*, 89–95.

[3] Savageau, M. A. (1976). *Biochemical systems analysis.* Addison-Wesley, London.

[4] Hofmeyr, J.-H. S. (1986). *Comp. Appl. Biosci. 2*, 5–11.

[5] Hofmeyr, J.-H. S. and Cornish-Bowden, A. (1991). *Eur. J. Biochem. 200*, 223–236.

[6] Hofmeyr, J.-H. S. and Cornish-Bowden, A. (1997). *Comp. Appl. Biosci. 13*, 377–385.

[7] Umbarger, H. E. (1958). *Science 123*, 848.

[8] Cornish-Bowden, A. (1995). *Fundamentals of enzyme kinetics.* Portland Press, London, 2nd edition.

[9] Hofmeyr, J. H. S. (1995). *J. Bioenerg. Biomembranes 27*, 479–490.

[10] Sauro, H. M. (1993). *Comp. Appl. Biosci. 9*, 441–450.

[11] Mendes, P. (1993). *Comp. Appl. Biosci. 9*, 563–571.

[12] Cascante, M. and Martí, E. (1997). Organization and Regulation of the Metabolic Factory. In Cornish-Bowden, A., editor, *New Beer in an Old Bottle: Eduard Buchner and the Growth of Biochemical Knowledge*, Col.lecció Oberta, pp. 199–214. Universitat de València, Valencia.

[13] Atkinson, D. E. (1977). *Cellular energy metabolism and its regulation.* Academic Press, New York.

[14] Koch, A. L. (1967). *J. Theor. Biol. 15*, 75–102.

[15] Fell, D. (1996). *Understanding the control of metabolism.* Portland Press, London.

[16] Hofmeyr, J.-H. (1997). Anaerobic Energy Metabolism in Yeast as a Supply-Demand System. In Cornish-Bowden, A., editor, *New Beer in an Old Bottle: Eduard Buchner and the Growth of Biochemical Knowledge*, Col.lecció Oberta, pp. 225–242. Universitat de València, Valencia.

[17] Cornish-Bowden, A., Hofmeyr, J.-H. S., and Cárdenas, M. L. (1995). *Bioorg. Chem. 23*, 439–449.

[18] Reder, C. (1988). *J. Theor. Biol. 135*, 175–201.

[19] Meléndez-Hevia, E. (1985). *J. Theor. Biol. 117*, 251–263.

[20] Meléndez-Hevia, E. and Torres, N. V. (1988). *J. Theor. Biol. 132*, 97–111.

[21] Meléndez-Hevia, E. (1990). *Biomed. Biochim. Acta 49*, 903–916.

[22] Meléndez-Hevia, E., Waddell, T. G., and Montero, F. (1994). *J. Theor. Biol. 166*, 201–220.

[23] Meléndez-Hevia, E., Waddell, T. G., and Cascante, M. (1996). *J. Mol. Evol. 43*, 293–303.

[24] Heinrich, R. H., Montero, F., Klipp, E., Waddell, T. G., and Meléndez-Hevia, E. (1997). *Eur. J. Biochem. 243*, 191–201.

[25] Waddell, T. G., Repovic, P., Meléndez-Hevia, E., Heinrich, R. H., and Montero, F. (1997). *Biochem. Educ. 25*, 204–205.

[26] Waddell, T. G., Repovic, P., Meléndez-Hevia, E., Heinrich, R. H., and Montero, F. (1999). *Biochem. Educ. 27*, 12–13.

[27] Hofmeyr, J. H. S. and Cornish-Bowden, A. (1996). Predicting Metabolic Pathway Kinetics with Control Analysis. In Westerhoff, H. V., Snoep, J. L., Wijker, J. E., Sluse, F. E., and Kholodenko, B. N., editors, *BioThermoKinetics of the Living Cell*, pp. 155–158. BioThermoKinetics Press, Amsterdam.

[28] Fell, D. A. and Snell, K. (1988). *Biochem. J. 256*, 97–101.

[29] Popova, S. V. and Sel'kov, E. E. (1975). *FEBS Lett. 53*, 269–273.

[30] Szedlacsek, S. (1999). Time-Dependent or Steady-State Control of Metabolic Systems? In Cornish-Bowden, A., editor, *Technological and Medical Implications of Metabolic Control Analysis*. Kluwer Academic Publishers, Dordrecht, in the press.

[31] Easterby, J. S. (1981). *Biochem. J. 199*, 155–161.

[32] Easterby, J. S. (1986). *Biochem. J. 233*, 871–875.

[33] Easterby, J. S. (1990). *Biochem. J. 269*, 255–259.

[34] Meléndez-Hevia, E., Torres, N. V., Sicilia, J., and Kacser, H. (1990). *Biochem. J. 265*, 195–202.

[35] Cascante, M., Torres, N. V., Franco, R., Meléndez-Hevia, E., and Canela, E. I. (1991). *Mol. Cell. Biochem. 101*, 83–91.

[36] Cascante, M., Meléndez-Hevia, E., Kholodenko, B., Sicilia, J., and Kacser, H. (1995). *Biochem. J. 308*, 895–899.

[37] Meléndez-Hevia, E., Sicilia, J., Ramos, M. T., Canela, E. I., and Cascante, M. (1996). *J. Theor. Biol. 182*, 333–339.

[38] Storer, A. C. and Cornish-Bowden, A. (1974). *Biochem. J. 141*, 205–209.

[39] Acerenza, L. (1993). *J. Theor. Biol. 165*, 63–85.

[40] Acerenza, L. (1996). *J. Theor. Biol. 182*, 277–283.

[41] Acerenza, L. (1999). Metabolic Control Design: Implications and Applications. In Cornish-Bowden, A., editor, *Technological and Medical Implications of Metabolic Control Analysis*. Kluwer Academic Publishers, Dordrecht, in the press.